

A Multi-Bound Robust Optimization Approach for Renewable-Based VPP Market Participation Considering Intra-Hourly Uncertainty Exposure

Hadi Nemati*, Álvaro Ortega, Enrique Lobato, Luis Rouco

Comillas Pontifical University, Institute for Research in Technology, Madrid, Spain

*Corresponding author

E-mail address: hnemati@comillas.edu

Abstract

With the ongoing transition of electricity markets worldwide from hourly to intra-hourly bidding, market participants—especially Renewable Energy Sources (RES)—gain improved opportunities to adjust energy and reserve schedules and to benefit from more accurate higher-resolution forecasts. However, this shift requires participants to update decision-making frameworks and to strengthen uncertainty management in order to fully exploit the new market potential. In particular, Renewable-Based Virtual Power Plants (RVPPs) aggregating dispatchable and non-dispatchable RES must account for these changes through market-oriented scheduling methods that efficiently address multiple uncertainties, including electricity prices, RES generation, and demand consumption. In this vein, this paper proposes a multi-bound robust optimization framework to simultaneously capture these uncertainties, explicitly incorporate intra-hourly variability, and differentiate the deviation levels (frequent, moderate deviations and rare, extreme ones) of uncertain parameters. The proposed approach yields less conservative and more implementable bidding and scheduling decisions, thus improving RVPP profitability in both energy and reserve markets. Simulation studies compare the proposed method with standard robust optimization and evaluate the operational, market-strategy, and economic impacts of quarter-hourly versus hourly market resolution. Results indicate that the normalized absolute differences, across different uncertainty-handling strategies, between hourly and 15-minute schedules are 18.0–34.2% for day-ahead traded energy, and 28.7–65.6% and 10.1–16.3% for upward and downward reserve traded in the secondary reserve market, respectively. Furthermore, relative to classic robust optimization, the proposed multi-bound approach increases profit by 24.9–49.2% across the considered strategies.

Keywords

Renewable-based virtual power plant, Multi-bound robust optimization, Intra-hourly uncertainty, energy and reserve markets

Nomenclature

Abbreviations

C&CG	Column & Constraint Generation	ND-RES	Non-Dispatchable Renewable Energy Sources
CVaR	Conditional Value-at-Risk	PV	Photovoltaic
D-RES	Dispatchable Renewable Energy Sources	RES	Renewable Energy Sources
DAM	Day-Ahead Market	RO	Robust Optimization
DRO	Distributed Robust Optimization	RVPP	Renewable-Based Virtual Power Plant
ESS	Energy Storage System	SO	Stochastic Optimization
EV	Electric Vehicle	SRM	Secondary Reserve Market
IGDT	Information Gap Decision Theory	VPP	Virtual Power Plant
MILP	Mixed Integer Linear Programming		

Indices and Sets

$t \in \mathcal{T}$	Set of time periods
$u \in \mathcal{U}$	Set of RVPP units, comprising ND-RESs ($r \in \mathcal{R}$), ESSs ($s \in \mathcal{S}$), D-RESs ($c \in \mathcal{C}$), and demands ($d \in \mathcal{D}$)
$k \in \mathcal{K}$	Set of uncertainty bounds in MBRO approach
$t \in \mathcal{T}_k$	Set of worst-case time periods for bound k
$\Xi^{F/S}$	Sets of first- and second-level decision variables of the RVPP operator

Parameters

C_u	Marginal operation cost of unit u	[€/MWh]
E_u	Rated energy capacity of unit u	[MWh]
P_u	Rated power capacity or power forecast of unit u	[MW]
R_u	Ramp rate of unit u	[MW/min]
T^{SR}	Secondary reserve activation time	[min]
β_u	Reserve provision limit factor of unit u	[%]
Γ_k	Uncertainty budget for bound k	[–]
Δt	Time step duration	[h]
η_u	Efficiency of unit u	[%]
λ_t	Forecast electricity market price during period t	[€/MW, €/MWh]

Variables

$e_{u,t}$	Stored energy level of unit u at the end of period t	[MWh]
p_t^{DA}	Power traded by the RVPP in the DAM during period t	[MW]
$p_{u,t}$	Power dispatch of unit u during period t	[MW]
r_t^{SR}	Reserve capacity traded by the RVPP in the SRM during period t	[MW]
$r_{u,t}$	Reserve contribution provided by unit u during period t	[MW]
σ_u	Fraction of unit u capacity allocated for reserve	[%]
$y_{k,t}$	Auxiliary variable for uncertainty bound k during period t	[MW, MWh]
$z_{k,t}$	Auxiliary variable for uncertainty budget of bound k during period t	[–]
ϕ_k	Dual variable associated with the uncertain parameters of bound k	[€, MW]
ζ_t	Dual variable associated with uncertain parameters during period t	[€, MW]
$v_{u,t}$	Binary commitment status of unit u during period t	[–]
$\chi_{u,k,t}$	Binary indicator for worst-case realization of unit u under bound k during period t	[–]

Superscripts and Accents

A^{DA}	Related to the DAM
A^{SR}	Related to the SRM
$A^{\uparrow}, A^{\downarrow}$	Upward and downward reserve directions
A^+, A^-	Charging and discharging states of ESSs
\tilde{A}	Median forecast value of an uncertain parameter
A^*	Optimal value of a variable
\hat{A}, \check{A}	Positive and negative deviations of an uncertain parameter from the forecast
\bar{A}, \underline{A}	Upper and lower bounds (e.g., limits or forecast bounds) of a parameter

1. Introduction

1.1. Motivation

Electricity markets worldwide are currently undergoing a fundamental structural transition toward higher temporal granularity, moving from traditional hourly settlements to sub-hourly (e.g., quarter-hourly) intervals. This shift is driven by evolving market rules aiming to harmonize market designs and, more critically, to facilitate the seamless integration of variable Renewable Energy Sources (RES) [1]. Within Europe, one recent example is the Spanish market's scheduled transition in October 2025, which replaces the standard 24 daily price points with 96 quarter-hourly intervals [2, 3]. The primary goal of this transition is to align market schedules more closely with physical grid operations, incentivizing this way participants to balance supply and demand in near real-time and reducing reliance on costly adjustment mechanisms.

Under this transformed regulatory framework, the core platform for energy trading, the Day-Ahead Market (DAM), evolves from the traditional 24-period structure to a higher resolution timeline divided into 96 quarter-hourly intervals, in which generation and demand agents submit bids for each 15-minute slot, after which the market operator establishes market-clearing prices that reflect the immediate volatility of the grid more accurately than hourly averages [4]. Parallel to energy trading, the Secondary Reserve Market (SRM), particularly for automatic frequency restoration reserve, remains the critical mechanism for the system operator to restore system frequency and power exchanges to scheduled values [5]. However, the technical requirements for providing reserve capacity are now tightly synchronized with the quarter-hourly energy settlement periods.

A Renewable-based Virtual Power Plant (RVPP) operates as a unified entity that aggregates diverse assets, ranging from stochastic Non-dispatchable RES (ND-RES) and controllable Dispatchable RES (D-RES) to Energy Storage System (ESS) and flexible demand, to provide grid services and enhance profitability [6]. For market participants, particularly RVPPs, this transition brings both opportunity and challenge. The shift to finer time resolutions exposes RVPPs to "intra-hourly" dynamics previously smoothed out in hourly models. While market structures have evolved to accommodate RES variability, traditional optimization models often lag behind, relying on coarse uncertainty handling approaches that miss rapid fluctuations in RES production, demand, and DAM/SRM prices at a 15-minute scale [7]. Consequently, fully leveraging high-resolution markets requires updating RVPP bidding strategies [8]. Specifically, uncertainty handling frameworks must be refined beyond hourly assumptions, ensuring that the RVPP can manage and profit from the granular volatility inherent in this new market era.

1.2. Literature Review

The participation of Virtual Power Plants (VPPs) in the DAM has been extensively researched, particularly regarding the management of uncertainties associated with RES production and demand. Numerous studies employ Robust Optimization (RO) and Stochastic Optimization (SO) techniques to address these

challenges [9–14]. For instance, Liu et al. [9] proposed a two-stage RO approach that incorporates a refined demand response strategy, solving the problem via the Column & Constraint Generation (C&CG) algorithm with fuzzy-based subproblems. Wu et al. [10] developed a two-stage Distributed RO (DRO) model for rural VPPs integrating biomass and RES, utilizing a dual vertices fixing algorithm to handle correlated wind and solar uncertainties. The integration of ESS was addressed by Feng et al. [11], who applied an improved nested C&CG algorithm within a two-stage DRO framework to manage power deviations. Beyond electricity, Li et al. [12] extended RO to multi-energy VPPs participating in both energy and peak-regulation markets. Falabretti et al. [13] utilized a Monte Carlo-based two-stage SO for RVPPs with Electric Vehicle (EV) charging stations, while Cao et al. [14] explored carbon trading flexibility using scenario-based DRO. However, a significant limitation of these works is the neglect of market price uncertainty, a factor that critically impacts VPP profitability.

To address this limitation, recent literature has incorporated market price uncertainty alongside generation variability [15–19]. Wang et al. [15] introduced a two-stage DRO model that handles DAM price uncertainty in the first stage and utilizes Conditional Value-at-Risk (CVaR) to manage real-time price risks. Incorporating risk preferences, Xiao et al. [17] proposed an SO framework capable of modeling both risk-seeking and risk-averse strategies, while Shafiekhani et al. [18] employed Information Gap Decision Theory (IGDT) to balance economic viability and emission minimization under different risk attitudes. Advanced bi-level structures have also been proposed; Afzali et al. [19] developed a risk-aware SO–RO strategy for energy and flexibility markets, reformulating the problem as a Mixed Integer Linear Programming (MILP) to ensure global optimality. Furthermore, hybrid uncertainty handling methods have emerged, such as the data-driven RO model by Ma et al. [20], which captures price uncertainty via data-driven techniques and physical uncertainties via RO. Others have extended these frameworks to price-maker VPPs [21] and low-carbon scheduling [22], simultaneously quantifying uncertainties in generation, load, and prices.

While the aforementioned studies focus primarily on energy trading, VPPs can also leverage flexible assets to provide ancillary services, enhancing system stability and their revenue [6, 23–32]. Yang et al. [6] utilized non-linear programming for joint participation in energy, reserve, and regulation markets, characterizing uncertainties via confidence intervals. Shang et al. [23] applied an interval probability method to manage volatility across emergency levels in frequency modulation markets. Feng et al. [24] proposed a chance-constrained DRO framework defining interval ambiguity sets for RES generation. Du et al. [25] modeled the physical-economic feasible region of VPPs within a two-stage optimization for joint markets, and Siqin et al. [26] addressed simultaneous energy, reserve, and carbon trading. Additionally, Esfahani et al. [27] focused on frequency regulation from aggregated small ESS, employing an SO–RO approach with CVaR to manage capacity and price risks. Nokandi et al. [28] developed a three-stage SO model incorporating intraday demand response exchanges, while Zamani et al. [29] applied point estimate methods for joint electrical and thermal scheduling. Li et al. [33] introduce a risk-aware SO framework for multi-market bidding that broadens the scope of uncertainty to encompass not only RES variability but also the compliance willingness of users. Robust frameworks have also been refined; Nemati et al. proposed methods capturing asymmetric uncertainties in sequential markets [30], handling non-linear couplings in simultaneous markets via flexible RO [31], and integrating concentrated solar power through reformulated two-stage RO [32].

As discussed above, the domain of hourly multi-market participation is quite mature, with sophisticated optimization techniques handling diverse uncertainties. However, the transition of electricity markets toward higher temporal resolution leaves existing hourly models insufficient for capturing intra-hourly dynamics. Limited research has been focused on addressing this shift [34–36]. Li et al. [34] proposed a DRO strategy for a 96-period market, but they simplified market prices to hourly resolution to aid convergence. Yuanyuan et al. [35] focused on a 96-period declaration strategy with flexible ramping products, yet their uncertainty modeling was limited to wind power. Wang et al. [36] utilized Italian market data to model hourly DAM

and 15-minute reserve markets but did not fully account for intra-hourly price and demand volatility. Consequently, there remains a critical gap for a holistic approach that enables VPP participation in high-resolution energy and reserve markets while comprehensively accounting for the intra-hourly exposure to uncertainties in market prices, RES generation, and demand. In this context, Table 1 contrasts the key features of this study against the reviewed literature.

To fill the identified gaps and align with the transition of electricity markets worldwide toward sub-hourly resolution, this paper proposes a novel bidding strategy for RVPP participation in the DAM and SRM. The core contribution is the development of a Multi-Bound Robust Optimization (MBRO) framework capable of simultaneously managing the multiple uncertainties inherent in electricity prices, ND-RES production, and demand. The concept of MBRO was developed in [37] to mitigate the inherent conservatism of classical RO theory [38]. The proposed MBRO framework in this paper fundamentally differs from the traditional RO approach by explicitly modeling intra-hourly uncertainty exposure. Standard RO formulations typically apply a single global robustness budget across the time horizon, often resulting in a binary outcome where specific time periods are fully protected against maximum possible deviations—leading to excessive conservatism—while remaining periods are treated optimistically with no protection once the budget is exhausted. In contrast, the proposed MBRO discretizes the uncertainty spectrum into distinct "bounds" corresponding to different deviation magnitudes. The RVPP operator can, in this way, define flexible robustness budgets for each bound rather than relying on a single global parameter. By assigning higher budgets to lower bounds (representing frequent, moderate deviations) and lower budgets to upper bounds (representing rare, extreme deviations), the formulation ensures broader protection across more time intervals without forcing the solution to accommodate the maximum protection for every period. The aim is to effectively balance risk and profitability to yield practical bidding decisions tailored to high-resolution markets. The study further details the mathematical proof for the linear reformulation of this bi-level MBRO problem and validates the approach through extensive comparisons with classic RO and hourly-resolution benchmarks.

1.3. Paper Contributions

The main contributions of this paper are outlined as follows:

- **Proposes an MBRO bidding framework for RVPP market participation:** This approach simultaneously handles multiple uncertainties related to electricity prices, ND-RES production, and demand consumption. Unlike classical RO, which often yields overly conservative solutions by treating all uncertainty realizations uniformly, the proposed MBRO formulation provides a more realistic representation of uncertainty. By distinguishing between frequent, moderate deviations and rare, extreme ones, the approach generates less conservative, more implementable schedules that enhance the profitability of the RVPP.
- **Addresses intra-hourly uncertainty exposure in market transitions:** The model aligns with the recent transition of electricity markets from hourly to finer temporal bidding structures. The study highlights that ignoring intra-hour uncertainty leads to a systematic misestimation of imbalance risks by smoothing out intra-hour volatility in RVPP trading and scheduling. This paper provides more realistic and granular bidding decisions for modern electricity markets by handling uncertainty at a quarter-hourly time resolution.
- **Quantifies the value of multi-bound robustness and granularity:** A rigorous comparative analysis against standard RO benchmarks is conducted across different uncertainty-handling strategies. It also quantifies the economic and technical impact of market time-resolution (15-min vs. hourly) on decision-making, offering insights into the trade-offs between computational complexity, uncertainty coverage, and profit maximization in the new market era.

Table 1: Comparison of the approach in this paper and recent literature.

Ref.	Market		Market resolution		Uncertainty		Intra-hourly	Uncertainty treatment		Method
	Energy	Reserve	24-period	96-period	Price	RES	Demand	uncertainty	Single-bound	
[9]	•					•			•	RO
[10, 11]	•		•			•			•	DRO
[12]	•		•			•	•		•	RO
[13]	•		•			•	•			SO
[14]	•		•			•	•		•	DRO
[15]	•		•			•			•	CVaR–DRO
[16, 17]	•		•			•	•			SO
[18]	•		•			•	•		•	IGDT
[19]	•		•			•	•		•	SO–RO
[20, 22]	•		•			•	•		•	RO
[21]	•		•			•	•		•	DRO
[6, 23]	•	•	•			•				Probability distribution
[24]	•	•	•			•				Chance constrained DRO
[25]	•	•	•			•	•			Chance constrained
[26]	•	•	•			•	•			DRO
[27]	•	•	•			•	•		•	SO–RO
[28, 29, 33]	•	•	•			•	•			SO
[30–32]	•	•	•			•	•		•	RO
[34]	•			•		•			•	DRO
[35]	•	•		•		•			•	DRO
[36]	•	•		•		•			•	RO
This paper	•	•		•	•	•	•	•	•	MBRO

The remainder of this paper is organized as follows. Section 2 defines the operational scope and problem statement. The mathematical formulation of the proposed MBRO strategy for the RVPP’s joint participation in the DAM and SRM is derived in Section 3. A comprehensive numerical analysis and discussion of the results are presented in Section 4. Finally, Section 5 summarizes the key findings and suggests potential directions for future research.

2. Problem Description

The operational framework of the proposed RVPP is conceptually illustrated in Figure 1. As depicted, the RVPP functions as a central aggregator that coordinates a diverse portfolio of assets, including D-RES (e.g., hydro plant), ND-RES (e.g., wind and solar Photovoltaic (PV)), demand, and ESS. The figure distinguishes between two primary interaction flows essential for the RVPP’s operation. First, the electrical energy flow (blue lines) represents the physical power exchange between the power grid and the internal assets. The RVPP facilitates the grid integration of ND-RES by balancing their variability with controllable dispatchable units and storage, with the aim to ensure technical feasibility and reliable demand satisfaction. Second, the data and decision flow (red dashed lines) represents the decision-making core where the RVPP operator gathers technical data and availability forecasts from internal units while simultaneously monitoring market conditions. Based on this information, the operator submits optimal bids to the DAM for energy trading and the SRM for ancillary services. In this framework, the RVPP is modeled as a price-taker and submits zero-price bids to ensure dispatch. The rationale for this assumption lies in the RVPP’s relatively small

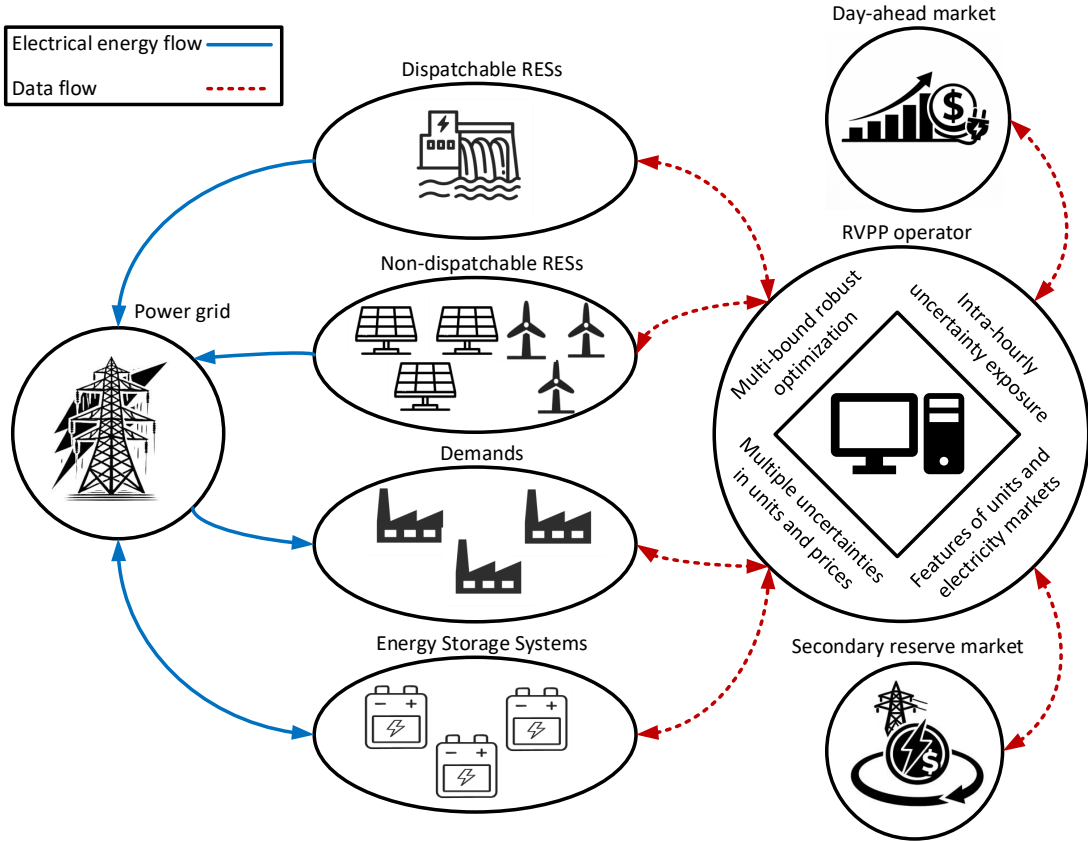


Figure 1: The operational framework of the proposed RVPP.

size compared to the grid size, as well as the economic characteristics of its aggregated assets, which are primarily ND-RES with low marginal operating costs. Once the markets clear, the operator disaggregates the commitments, communicating specific dispatch set-points back to the internal units to maintain the schedule.

A critical challenge for the RVPP operator is managing the multiple uncertainties in units and prices highlighted in the optimization block of Figure 1. To maximize profitability while ensuring robustness, the operator must account for stochasticity in ND-RES production, demand consumption, and market prices. While recent literature suggests that flexible RO allows operators to adjust conservatism via uncertainty budgets [20, 22, 30, 36], standard RO approaches often treat all deviations uniformly. This can lead to overly conservative schedules that fail to capture the nuances of more granular bidding structures. To address these limitations, this study proposes an MBRO approach, mathematically formulated in the following section. Unlike classical methods, MBRO segments the uncertainty spectrum into distinct bounds (e.g., frequent small deviations vs. rare extreme events). This granular handling of uncertainty allows the RVPP to prioritize frequent deviations over rare sharp ones, resulting in less conservative bidding strategies that maintain computational efficiency and are better aligned with the high-resolution requirements of modern energy and reserve markets.

3. Formulation

This section details the mathematical framework of the proposed MBRO approach for the RVPP operation. Section 3.1 first outlines the deterministic model for participation in the DAM and SRM in line with existing literature [20, 22, 30, 31, 36]. Subsequently, to effectively address the inherent volatility of electricity prices, generation from ND-RES, and demand consumption, Section 3.2 introduces the proposed MBRO framework as a novel contribution of this work.

3.1. Deterministic Problem

3.1.1. Objective Function

The objective function defined in (1) serves to maximize the RVPP's total operational profit derived from participation in both the DAM and the SRM. This formulation aggregates revenues from energy trading and bidirectional reserve provision, subtracting the operational expenditures associated with D-RESs, ND-RESs, and ESSs.

$$\max_{\Xi^F} \sum_{t \in \mathcal{T}} \lambda_t^{DA} p_t^{DA} \Delta t + \sum_{t \in \mathcal{T}} [\lambda_t^{SR,\uparrow} r_t^{SR,\uparrow} + \lambda_t^{SR,\downarrow} r_t^{SR,\downarrow}] - \sum_{t \in \mathcal{T}} \sum_{c \in \mathcal{C}} C_c p_{c,t} \Delta t - \sum_{t \in \mathcal{T}} \sum_{r \in \mathcal{R}} C_r p_{r,t} \Delta t - \sum_{t \in \mathcal{T}} \sum_{s \in \mathcal{S}} C_s p_{s,t} \Delta t \quad (1)$$

3.1.2. Supply–Demand Constraints

The fundamental requirement for the RVPP to meet its market obligations is the preservation of power balance at every time step. The supply–demand constraint (2) is thus defined to ensure that the RVPP's aggregated output matches its commitment regardless of whether secondary reserves are activated in the upward or downward direction, or remain inactive. To implement this, the model employs the reserve state vectors, $\mathbf{r}_t^{SR} = \{r_t^{SR,\uparrow}, -r_t^{SR,\downarrow}, 0\}$ for the RVPP, and $\mathbf{r}_{u,t} = \{r_{u,t}^{\uparrow}, -r_{u,t}^{\downarrow}, 0\}$ for individual assets $u \in \mathcal{U}$, including ND-RESs, ESSs, D-RESs, and demands. Thus, equation (2) describes a system of three distinct balance equations that fully capture the deterministic response required for each activation scenario [31].

$$\sum_{r \in \mathcal{R}} [p_{r,t} + \mathbf{r}_{r,t}] + \sum_{s \in \mathcal{S}} [p_{s,t} + \mathbf{r}_{s,t}] + \sum_{c \in \mathcal{C}} [p_{c,t} + \mathbf{r}_{c,t}] - \sum_{d \in \mathcal{D}} [p_{d,t} - \mathbf{r}_{d,t}] = p_t^{DA} + \mathbf{r}_t^{SR}; \quad \forall t \quad (2)$$

3.1.3. Dispatchable Unit Constraints

In this study, D-RES units are defined as renewable energy assets that can be operated in a controllable manner, similar to conventional thermal units. These resources include units such as hydro plants and can be scheduled by the RVPP within their operational limits to provide both energy and reserve. To model this controllability, constraints (3a) and (3b) define the operational limits for energy and reserve provision, contingent on the binary commitment variable $v_{c,t}$. Constraint (3c) ensures compliance with daily energy production limits, often dictated by seasonal water management policies (e.g., for hydro plants). Finally, temporal constraints regarding minimum up and down times are omitted here for brevity but follow the standard MILP formulation presented in [39].

$$p_{c,t} + r_{c,t}^{\uparrow} \leq \bar{P}_c v_{c,t}; \quad \forall c, t \quad (3a)$$

$$\underline{P}_c v_{c,t} \leq p_{c,t} - r_{c,t}^{\downarrow}; \quad \forall c, t \quad (3b)$$

$$\sum_{t \in \mathcal{T}} [p_{c,t} \Delta t + r_{c,t}^{\uparrow}] \leq \bar{E}_c; \quad \forall c \quad (3c)$$

3.1.4. Non-dispatchable Unit Constraints

The category of ND-RES includes stochastic assets like wind and solar PV, where the maximum output is mostly determined by meteorological forecasts rather than operator dispatch. Despite this, they can participate in the SRM by modulating curtailment levels: downward reserve is provided by reducing output, whereas upward reserve is available when the unit is pre-curtailed below its available potential [40, 41]. In the model, Constraint (4a) caps production at the forecasted limit $P_{r,t}$, while Constraint (4b) defines the lower feasibility bounds for simultaneous energy and reserve schedules.

$$p_{r,t} + r_{r,t}^{\uparrow} \leq P_{r,t} ; \quad \forall r, t \quad (4a)$$

$$P_r \leq p_{r,t} - r_{r,t}^{\downarrow} ; \quad \forall r, t \quad (4b)$$

3.1.5. Demand Constraints

Electrical demand represents a source of both flexibility and stochasticity within the RVPP portfolio [24]. The feasible operating domain, which accounts for simultaneous power consumption and reserve provision, is established by constraints (5a) and (5b), where the lower consumption limit is governed by forecast uncertainty. The minimum energy requirement over the scheduling horizon is enforced by constraint (5c).

$$P_{d,t} \leq p_{d,t} - r_{d,t}^{\uparrow} ; \quad \forall d, t \quad (5a)$$

$$p_{d,t} + r_{d,t}^{\downarrow} \leq \bar{P}_d ; \quad \forall d, t \quad (5b)$$

$$E_d \leq \sum_{t \in \mathcal{T}} [p_{d,t} \Delta t - r_{d,t}^{\uparrow}] ; \quad \forall d \quad (5c)$$

3.1.6. ESS Constraints

ESSs are rapidly gaining popularity as flexibility provision assets, due to their capability to efficiently mitigate the intermittency of ND-RESs, among other interesting features. The mathematical framework governing ESS operation is presented in (6), enabling simultaneous optimization of energy arbitrage and reserve provision [32]. Constraints (6a)–(6d) establish the operational boundaries for ESS power and reserve, ensuring that sufficient capacity is maintained for both upward and downward reserve provision in both charging (+) and discharging (−) states. The binary variable $v_{s,t}$ is utilized to explicitly differentiate between the charging and discharging states, thus preventing simultaneous operation. The resulting net power output and total reserve capacity are aggregated in (6e)–(6g). Regarding energy management, equation (6h) tracks the state of charge dynamics, while constraint (6i) imposes a daily cyclic balance by equating the initial and final stored energy. Note that this constraint can be relaxed according to RVPP operator needs. The allocation of storage capacity for upward and downward reserves is governed by coefficients σ_s^{\uparrow} and σ_s^{\downarrow} in (6j)–(6k). Finally, constraint (6l) adjusts the feasible energy limits to account for the energy allocated to reserve capacity.

$$P_s^+ v_{s,t} \leq p_{s,t}^+ - r_{s,t}^{+,\uparrow} ; \quad \forall s, t \quad (6a)$$

$$p_{s,t}^+ + r_{s,t}^{+,\downarrow} \leq \bar{P}_s^+ v_{s,t} ; \quad \forall s, t \quad (6b)$$

$$P_s^- v_{s,t} + r_{s,t}^{-,\uparrow} \leq \bar{P}_s^- (1 - v_{s,t}) ; \quad \forall s, t \quad (6c)$$

$$P_s^- (1 - \nu_{s,t}) \leq p_{s,t}^- - r_{s,t}^{-\downarrow} ; \quad \forall s, t \quad (6d)$$

$$p_{s,t} = p_{s,t}^- - p_{s,t}^+ ; \quad \forall s, t \quad (6e)$$

$$r_{s,t}^{\uparrow} = r_{s,t}^{+\uparrow} + r_{s,t}^{-,\uparrow} ; \quad \forall s, t \quad (6f)$$

$$r_{s,t}^{\downarrow} = r_{s,t}^{+\downarrow} + r_{s,t}^{-,\downarrow} ; \quad \forall s, t \quad (6g)$$

$$e_{s,t} = e_{s,t-1} + p_{s,t}^+ \eta_s^+ \Delta t - \frac{p_{s,t}^- \Delta t}{\eta_s^-} ; \quad \forall s, t \setminus \{1\} \quad (6h)$$

$$e_{s,1} = e_{s,|\mathcal{T}|} ; \quad \forall s \quad (6i)$$

$$\sum_{t \in \mathcal{T}} \frac{r_{s,t}^{\uparrow} \Delta t}{\eta_s^-} \leq \sigma_s^{\uparrow} (\bar{E}_s - \underline{E}_s) ; \quad \forall s \quad (6j)$$

$$\sum_{t \in \mathcal{T}} r_{s,t}^{\downarrow} \eta_s^+ \Delta t \leq \sigma_s^{\downarrow} (\bar{E}_s - \underline{E}_s) ; \quad \forall s \quad (6k)$$

$$\underline{E}_s + \sigma_s^{\downarrow} (\bar{E}_s - \underline{E}_s) \leq e_{s,t} \leq \bar{E}_s - \sigma_s^{\downarrow} (\bar{E}_s - \underline{E}_s) ; \quad \forall s, t \quad (6l)$$

3.1.7. Reserve Provision Constraints

Although the energy production limits are technology-specific, the mathematical framework governing reserve provision is unified across the RVPP portfolio. Constraints (7a) and (7b) determine the permissible upward and downward reserve capacity for each asset $u \in \mathcal{U}$ that comprises the RVPP portfolio. This reserve capacity is strictly bounded by their ramp-rate characteristics and the secondary reserve activation time. Constraints (7c) and (7d) cap the reserve contribution based on the unit's maximum electrical rating and the reserve provision limit factors assigned by the RVPP operator [31].

$$r_{u,t}^{\uparrow} \leq T^{SR} R_u^{\uparrow} ; \quad \forall u, t \quad (7a)$$

$$r_{u,t}^{\downarrow} \leq T^{SR} R_u^{\downarrow} ; \quad \forall u, t \quad (7b)$$

$$r_{u,t}^{\uparrow} \leq \beta_u^{\uparrow} \bar{P}_u ; \quad \forall u, t \quad (7c)$$

$$r_{u,t}^{\downarrow} \leq \beta_u^{\downarrow} \bar{P}_u ; \quad \forall u, t \quad (7d)$$

3.2. Multi-Bound Robust Model

The deterministic formulation in Section 3.1 assumes perfect foresight, neglecting the inherent volatility of market prices and asset energy outputs. However, uncertainty in electricity and reserve prices, as well as variations in ND-RES generation and demand, can significantly impact the RVPP's financial performance. To mitigate these risks, the optimization problem is extended to an MBRO framework in Section 3.2.1. This is formulated as a bi-level problem: the first level maximizes the RVPP's objective function analogous to the deterministic model, while the second level minimizes the RVPP's profit by identifying the worst-case realization of uncertain parameters within defined bounds. Unlike traditional RO, which typically

defines a single interval for uncertainty (often leading to overly conservative solutions dominated by extreme scenarios), the MBRO framework segments the uncertainty spectrum into distinct bounds (e.g., deviation levels). By assigning specific budgets to these separate bounds, the model captures a more granular profile of risk. To solve the resulting bi-level problem efficiently with standard optimization tools, the inner worst-case (second-level) problem is reformulated into an equivalent tractable form, enabling a single-level MILP implementation. Section 3.2.2 details this reformulation of the second-level uncertainty problem. Finally, Section 3.2.3 presents the final MILP formulation of the MBRO model as a single-level problem solvable by commercial MILP solvers.

3.2.1. Bi-Level Formulation

The bi-level MBRO problem for the RVPP's participation in the DAM and SRM is formulated in (8)–(9). The objective function (8) seeks to maximize the base deterministic profit (represented by the first two lines, which account for expected market revenues based on price forecasts and unit operational costs) while explicitly subtracting the worst-case revenue loss caused by electricity price uncertainty in the third line. The set of first-level decision variables, Ξ^F , remains consistent with the deterministic model presented in Section 3.1. The worst-case realization of market prices is determined by the inner maximization problem, which is performed over the sets of worst-case time periods for DAM and SRM prices ($\mathcal{T}_k^{DA}, \mathcal{T}_k^{SR,\uparrow}, \mathcal{T}_k^{SR,\downarrow}$). The cardinality of these sets is equal to the value of the assigned uncertainty budgets ($\Gamma_k^{DA}, \Gamma_k^{SR,\uparrow}, \Gamma_k^{SR,\downarrow}$). These budgets are defined over the 96 quarter-hourly intervals of the daily horizon and constrain the number of time periods in which the uncertain parameter is allowed to deviate to the level associated with a specific bound k . Crucially, to ensure logical consistency, the summation of budgets across all bounds for a given parameter is limited to 96. This constraint enforces mutual exclusivity, ensuring that any specific time period can be assigned to at most one deviation level. This flexibility allows the operator to shape a less conservative uncertainty distribution—for example, by assigning larger budgets to frequent, minor deviations and restricting extreme deviations to a few rare instances. The uncertainty in DAM electricity prices is characterized by asymmetric intervals, expressed as $\lambda_t^{DA} \in [\tilde{\lambda}_t^{DA} - \check{\lambda}_{k,t}^{DA}, \tilde{\lambda}_t^{DA} + \hat{\lambda}_{k,t}^{DA}]$, where the magnitudes of positive and negative deviations, $\hat{\lambda}_{k,t}^{DA}$ and $\check{\lambda}_{k,t}^{DA}$, are generally distinct. Within these bounds, the determination of the worst-case price is contingent on the RVPP's net position in the market: a negative deviation constitutes the worst-case scenario when the portfolio is selling energy, whereas a positive deviation represents the worst case during energy purchase intervals. Conversely, for secondary reserve prices, only negative deviations are relevant to the robust analysis, as formulated by the intervals ($\lambda_t^{SR,\uparrow} \in [\lambda_t^{SR,\uparrow} - \check{\lambda}_{k,t}^{SR,\uparrow}, \lambda_t^{SR,\uparrow}]$ and $\lambda_t^{SR,\downarrow} \in [\lambda_t^{SR,\downarrow} - \check{\lambda}_{k,t}^{SR,\downarrow}, \lambda_t^{SR,\downarrow}]$). By focusing on these adverse deviations only, the model ensures that the optimization problem accurately reflects the worst-case conditions defined by the chosen uncertainty budgets, ignoring favorable deviations that would increase the RVPP's profit.

$$\begin{aligned}
& \max_{\Xi^F} \left\{ \sum_{t \in \mathcal{T}} \left[\tilde{\lambda}_t^{DA} p_t^{DA} \Delta t + \lambda_t^{SR,\uparrow} r_t^{SR,\uparrow} + \lambda_t^{SR,\downarrow} r_t^{SR,\downarrow} \right] \right. \\
& - \sum_{t \in \mathcal{T}} \sum_{r \in \mathcal{R}} C_r p_{r,t} \Delta t - \sum_{t \in \mathcal{T}} \sum_{s \in \mathcal{S}} C_s p_{s,t} \Delta t - \sum_{t \in \mathcal{T}} \sum_{c \in \mathcal{C}} C_c p_{c,t} \Delta t \\
& \left. - \max_{\{\mathcal{T}_k^{DA}, \mathcal{T}_k^{SR,\uparrow}, \mathcal{T}_k^{SR,\downarrow}\}} \left\{ \sum_{t \in \mathcal{T}_k^{DA}} \sum_{k \in \mathcal{K}} \check{\lambda}_{k,t}^{DA} y_{k,t}^{DA} + \sum_{t \in \mathcal{T}_k^{SR,\uparrow}} \sum_{k \in \mathcal{K}} \check{\lambda}_{k,t}^{SR,\uparrow} r_t^{SR,\uparrow} + \sum_{t \in \mathcal{T}_k^{SR,\downarrow}} \sum_{k \in \mathcal{K}} \check{\lambda}_{k,t}^{SR,\downarrow} r_t^{SR,\downarrow} \right\} \right\} \quad (8)
\end{aligned}$$

The constraints governing the proposed bi-level MBRO framework are detailed in (9). Constraint (9a) addresses the asymmetric characteristics of DAM price uncertainty through the positive auxiliary variable $y_{k,t}^{DA}$. By distinguishing between positive ($\hat{\lambda}_{k,t}^{DA}$) and negative ($\check{\lambda}_{k,t}^{DA}$) price deviations, this variable effectively models the worst-case price realization contingent on the direction of the RVPP's energy trade in each period [32]. The uncertainty associated with ND-RES generation and demand consumption is managed by equations (9b) and (9c), respectively. These constraints incorporate specific uncertainty bounds to account for scenarios that worsen the objective function: ND-RES production is modeled with a focus on potential negative deviations ($P_{r,t} \in [\bar{P}_{r,t} - \check{P}_{r,k,t}, \bar{P}_{r,t}]$), whereas demand is modeled to account for potential positive deviations ($P_{d,t} \in [P_{d,t}, P_{d,t} + \hat{P}_{d,k,t}]$). The worst-case realizations for these parameters are determined by inner-level maximization problems performed over the sets $\mathcal{T}_{r,k}$ and $\mathcal{T}_{d,k}$, whose cardinalities, as discussed earlier, are equal to the uncertainty budgets $\Gamma_{r,k}$ and $\Gamma_{d,k}$ for each bound k . Consequently, constraints (9b) and (9c) apply the respective deviations (i.e., to reduce $\check{P}_{r,k,t'}$ and/or to increase $\hat{P}_{d,k,t'}$) to the forecast reference only if the index t' matches the current period t and simultaneously belongs to the selected worst-case set (i.e., $t' = t$ and $t' \in \mathcal{T}_{r,k}$ or $t' \in \mathcal{T}_{d,k}$). Finally, all deterministic constraints from Section 3.1 that remain unchanged under uncertainty are integrated in (9d).

$$-\frac{\check{\lambda}_{k,t}^{DA}}{\hat{\lambda}_{k,t}^{DA}} y_{k,t}^{DA} \leq p_t^{DA} \Delta t \leq y_{k,t}^{DA}; \quad \forall k, t \in \mathcal{K}, \mathcal{T} \quad (9a)$$

$$p_{r,t} + r_{r,t}^{\uparrow} \leq \bar{P}_{r,t} - \max_{\{\mathcal{T}_{r,k}\}} \left\{ \sum_{t' \in \mathcal{T}_{r,k}, t' = t} \sum_{k \in \mathcal{K}} \check{P}_{r,k,t'} \right\}; \quad \forall r, t \in \mathcal{R}, \mathcal{T} \quad (9b)$$

$$p_{d,t} - r_{d,t}^{\uparrow} \geq P_{d,t} + \max_{\{\mathcal{T}_{d,k}\}} \left\{ \sum_{t' \in \mathcal{T}_{d,k}, t' = t} \sum_{k \in \mathcal{K}} \hat{P}_{d,k,t'} \right\}; \quad \forall d, t \in \mathcal{D}, \mathcal{T} \quad (9c)$$

$$(2), (3), (4b), (5b)–(5c), (6), (7); \quad (9d)$$

3.2.2. Inner Problems Reformulation

The maximization term in the third line of the objective function (8) (the protection function) conceptually identifies the worst-case scenario via time sets $\mathcal{T}_k^{DA}, \mathcal{T}_k^{SR,\uparrow}, \mathcal{T}_k^{SR,\downarrow}$; however, since these sets are not predetermined, their selection logic must be recast as an equivalent linear optimization problem to facilitate the derivation of the final robust formulation [38]. Specifically, set membership is represented through positive auxiliary variables in the linear problem, whose optimal values yield the same worst-case choice as the original set-based definition by limiting their allowable deviations across time periods and within each bound. To achieve this, by treating the optimal values of the upper-level variables $(y_{k,t}^{DA*}, r_t^{SR,\uparrow*}, r_t^{SR,\downarrow*})$ as fixed parameters in the lower-level problem and applying Proposition 1 (see Appendix), the protection function in (8) is transformed into the linear problem (10). In this formulation, constraints (10b)–(10d) restrict the summation of each of the positive auxiliary variables $z_{k,t}^{DA}, z_{k,t}^{SR,\uparrow}$, and $z_{k,t}^{SR,\downarrow}$ over all time periods for each uncertainty bound k to the corresponding uncertainty budgets $\Gamma_k^{DA}, \Gamma_k^{SR,\uparrow}$, and $\Gamma_k^{SR,\downarrow}$, respectively. Simultaneously, constraints (10e)–(10g) ensure that the summation of these auxiliary variables across all bounds for any given time period does not exceed 1. This linear structure mathematically replicates the mutual exclusivity of the worst-case sets, ensuring that the optimal value of (10a) matches the protection

function in (8). The dual variables associated with each constraint are defined alongside these equations and are subsequently utilized in Section 3.2.3 to derive the final MILP formulation.

$$\max \left\{ \sum_{t \in \mathcal{T}} \sum_{k \in \mathcal{K}} \check{\lambda}_{k,t}^{DA} y_{k,t}^{DA*} z_{k,t}^{DA} + \sum_{t \in \mathcal{T}} \sum_{k \in \mathcal{K}} \check{\lambda}_{k,t}^{SR,\uparrow} r_t^{SR,\uparrow*} z_{k,t}^{SR,\uparrow} + \sum_{t \in \mathcal{T}} \sum_{k \in \mathcal{K}} \check{\lambda}_t^{SR,\downarrow} r_t^{SR,\downarrow*} z_{k,t}^{SR,\downarrow} \right\} \quad (10a)$$

st.

$$\sum_{t \in \mathcal{T}} z_{k,t}^{DA} \leq \Gamma_k^{DA} : \phi_k^{DA} ; \quad \forall k \in \mathcal{K} \quad (10b)$$

$$\sum_{t \in \mathcal{T}} z_{k,t}^{SR,\uparrow} \leq \Gamma_k^{SR,\uparrow} : \phi_k^{SR,\uparrow} ; \quad \forall k \in \mathcal{K} \quad (10c)$$

$$\sum_{t \in \mathcal{T}} z_{k,t}^{SR,\downarrow} \leq \Gamma_k^{SR,\downarrow} : \phi_k^{SR,\downarrow} ; \quad \forall k \in \mathcal{K} \quad (10d)$$

$$0 \leq \sum_{k \in \mathcal{K}} z_{k,t}^{DA} \leq 1 : \zeta_t^{DA} ; \quad \forall t \in \mathcal{T} \quad (10e)$$

$$0 \leq \sum_{k \in \mathcal{K}} z_{k,t}^{SR,\uparrow} \leq 1 : \zeta_t^{SR,\uparrow} ; \quad \forall t \in \mathcal{T} \quad (10f)$$

$$0 \leq \sum_{k \in \mathcal{K}} z_{k,t}^{SR,\downarrow} \leq 1 : \zeta_t^{SR,\downarrow} ; \quad \forall t \in \mathcal{T} \quad (10g)$$

The protection function describing the uncertainty of ND-RES electrical production in constraint (9b) (the maximization term on the right-hand side) is recast as the linear formulation (11) by applying Proposition 2 (see Appendix). To achieve the same worst-case selection logic as in (9b), the optimization problem (11) is defined individually for each time period t and ND-RES unit r [32]. The objective function (11a) maximizes the production deviation for the current period $t' = t$. Constraint (11b) ensures that the sum of the auxiliary variable $z_{r,k,(t'=t)}$ for the current period and the aggregate optimal values of variables from other protection functions ($z_{r,k,t'}^*$ where $t' \neq t$) remains within the limit $\Gamma_{r,k}$. Note that the variables $z_{r,k,t'}^*$ correspond to other protection functions (where $t' \neq t$) and are therefore treated as parameters in this constraint. Furthermore, the summation of the auxiliary variable $z_{r,k,(t'=t)}$ across all uncertainty bounds is limited to 1 by constraint (11c). The equivalent linear formulation for the demand uncertainty protection function in constraint (9c) follows an identical derivation and is omitted here for brevity.

$$\max \sum_{k \in \mathcal{K}} \check{P}_{r,k,(t'=t)} z_{r,k,(t'=t)} ; \quad \forall r, t \in \mathcal{R}, \mathcal{T} \quad (11a)$$

st.

$$z_{r,k,(t'=t)} + \sum_{t' \neq t} z_{r,k,t'}^* \leq \Gamma_{r,k} : \phi_{r,k} ; \quad \forall k \in \mathcal{K} \quad (11b)$$

$$0 \leq \sum_{k \in \mathcal{K}} z_{r,k,(t'=t)} \leq 1 : \zeta_{r,t} ; \quad (11c)$$

3.2.3. MILP Formulation

By leveraging strong duality theory [42], the inner linear maximization problems defined in (10) and (11) (as well as the analogous formulation for demand uncertainty) are replaced by their respective dual problems. Substituting the dual forms directly into the objective function (8) and constraints (9b) and (9c) yields the final single-level MILP formulation presented in (12). In this formulation, the objective function (12a) retains the deterministic profit terms in its first two lines, while the third line explicitly penalizes the objective function for the worst-case revenue losses arising from DAM and SRM price uncertainties. Constraint (12b) replicates the asymmetric price logic from (9a), and constraints (12c)–(12e) enforce the dual restrictions corresponding to the price uncertainty problem defined in (10).

The worst-case limits for ND-RES production are governed by constraints (12f)–(12j). Specifically, constraint (12f) defines the robust production upper bound. To model the discrete logical condition where the remaining budget term ($\Gamma_{r,k} - \sum_{r' \neq t} z_{r,k,r'}^*$) only corresponds to 0 or 1, the binary variable $\chi_{r,k,t}$ is introduced. Consequently, the positive auxiliary variable $y_{r,k,t}$ is established in (12f) and bounded via constraint (12g) using the Big-M method [42], thus linearizing the dual term $\sum_{k \in \mathcal{K}} \chi_{r,k,t} \phi_{r,k} + \zeta_{r,t}$. To ensure logical consistency, constraint (12h) enforces mutual exclusivity, ensuring only one uncertainty bound is active per time period, while constraint (12i) ensures the total number of active worst-case periods for each bound k matches the assigned uncertainty budget. Constraint (12j) represents the standard dual constraints derived from the ND-RES protection function (11). Similarly, constraints (12k)–(12o) manage demand uncertainty. These follow the same structural logic as the ND-RES constraints, with the primary distinction being the direction of the worst-case deviation. The domains of all positive auxiliary variables are defined in (12p)–(12q), and the remaining deterministic constraints are consolidated in (12r). Critically, this refined MILP framework allows for the flexible management of multiple uncertainty sources and enables the selection of distinct conservatism levels across different bounds via the uncertainty budgets.

$$\begin{aligned}
\max_{\Xi^F, \Xi^S} & \left\{ \sum_{t \in \mathcal{T}} \left[\tilde{\lambda}_t^{DA} p_t^{DA} \Delta t + \tilde{\lambda}_t^{SR,\uparrow} r_t^{SR,\uparrow} + \tilde{\lambda}_t^{SR,\downarrow} r_t^{SR,\downarrow} \right] \right. \\
& - \sum_{t \in \mathcal{T}} \sum_{r \in \mathcal{R}} C_r p_{r,t} \Delta t - \sum_{t \in \mathcal{T}} \sum_{s \in \mathcal{S}} C_s p_{s,t} \Delta t - \sum_{t \in \mathcal{T}} \sum_{c \in \mathcal{C}} C_c p_{c,t} \Delta t \\
& \left. - \sum_{k \in \mathcal{K}} \left[\Gamma_k^{DA} \phi_k^{DA} + \Gamma_k^{SR,\uparrow} \phi_k^{SR,\uparrow} + \Gamma_k^{SR,\downarrow} \phi_k^{SR,\downarrow} \right] - \sum_{t \in \mathcal{T}} \left[\zeta_t^{DA} + \zeta_t^{SR,\uparrow} + \zeta_t^{SR,\downarrow} \right] \right\} \tag{12a}
\end{aligned}$$

st.

$$-\frac{\tilde{\lambda}_{k,t}^{DA}}{\tilde{\lambda}_{k,t}^{DA}} y_{k,t}^{DA} \leq p_t^{DA} \Delta t \leq y_{k,t}^{DA}; \quad \forall k, t \in \mathcal{K}, \mathcal{T} \tag{12b}$$

$$\phi_k^{DA} + \zeta_t^{DA} \geq \tilde{\lambda}_{k,t}^{DA} y_{k,t}^{DA}; \quad \forall k, t \in \mathcal{K}, \mathcal{T} \tag{12c}$$

$$\phi_k^{SR,\uparrow} + \zeta_t^{SR,\uparrow} \geq \tilde{\lambda}_{k,t}^{SR,\uparrow} r_t^{SR,\uparrow}; \quad \forall k, t \in \mathcal{K}, \mathcal{T} \tag{12d}$$

$$\phi_k^{SR,\downarrow} + \zeta_t^{SR,\downarrow} \geq \tilde{\lambda}_{k,t}^{SR,\downarrow} r_t^{SR,\downarrow}; \quad \forall k, t \in \mathcal{K}, \mathcal{T} \tag{12e}$$

$$\begin{aligned}
p_{r,t} + r_{r,t}^\uparrow &\leq \bar{P}_{r,t} - \sum_{k \in \mathcal{K}} \chi_{r,k,t} \phi_{r,k} - \zeta_{r,t} = \bar{P}_{r,t} - \sum_{k \in \mathcal{K}} y_{r,k,t} ; & \forall r, t \in \mathcal{R}, \mathcal{T} & (12f) \\
\phi_{r,k} + \zeta_{r,t} - M(1 - \chi_{r,k,t}) &\leq y_{r,k,t} \leq M\chi_{r,k,t} ; & \forall r, k, t \in \mathcal{R}, \mathcal{K}, \mathcal{T} & (12g) \\
\sum_{k \in \mathcal{K}} \chi_{r,k,t} &\leq 1 ; & \forall r, t \in \mathcal{R}, \mathcal{T} & (12h) \\
\sum_{t \in \mathcal{T}} \chi_{r,k,t} &= \Gamma_{r,k} ; & \forall r, k \in \mathcal{R}, \mathcal{K} & (12i) \\
\phi_{r,k} + \zeta_{r,t} &\geq \check{P}_{r,k,t} ; & \forall r, k, t \in \mathcal{R}, \mathcal{K}, \mathcal{T} & (12j) \\
p_{d,t} - r_{d,t}^\uparrow &\geq P_{d,t} + \sum_{k \in \mathcal{K}} \chi_{d,k,t} \phi_{d,k} + \zeta_{d,t} = P_{d,t} + \sum_{k \in \mathcal{K}} y_{d,k,t} ; & \forall d, k, t \in \mathcal{D}, \mathcal{K}, \mathcal{T} & (12k) \\
\phi_{d,k} + \zeta_{d,t} - M(1 - \chi_{d,k,t}) &\leq y_{d,k,t} \leq M\chi_{d,k,t} ; & \forall d, k, t \in \mathcal{D}, \mathcal{K}, \mathcal{T} & (12l) \\
\sum_{k \in \mathcal{K}} \chi_{d,k,t} &\leq 1 ; & \forall d, t \in \mathcal{D}, \mathcal{T} & (12m) \\
\sum_{t \in \mathcal{T}} \chi_{d,k,t} &= \Gamma_{d,k} ; & \forall d, k \in \mathcal{D}, \mathcal{K} & (12n) \\
\phi_{d,k} + \zeta_{d,t} &\geq \hat{P}_{d,k,t} ; & \forall d, k, t \in \mathcal{D}, \mathcal{K}, \mathcal{T} & (12o) \\
\phi_k^{DA}, \phi_k^{SR,\uparrow}, \phi_k^{SR,\downarrow}, \zeta_t^{DA}, \zeta_t^{SR,\uparrow}, \zeta_t^{SR,\downarrow}, y_{k,t}^{DA} &\geq 0 ; & \forall k, t \in \mathcal{K}, \mathcal{T} & (12p) \\
\phi_{r,k}, \phi_{d,k}, \zeta_{r,t}, \zeta_{d,t}, y_{r,k,t}, y_{d,k,t} &\geq 0 ; & \forall r, d, k, t \in \mathcal{R}, \mathcal{D}, \mathcal{K}, \mathcal{T} & (12q) \\
(2), (3), (4b), (5b)–(5c), (6), (7) ; & & & (12r)
\end{aligned}$$

Figure 2 summarizes the overall workflow of the approach presented in this section: it outlines the deterministic RVPP formulation and the main steps leading to the MBRO model and its final single-level MILP. The figure also highlights the key characteristics enabled by the MBRO approach. The advantages of this proposed MBRO approach—specifically its ability to yield less conservative and more realistic solutions compared to classical robust optimization—are rigorously validated through the case studies presented in Section 4.

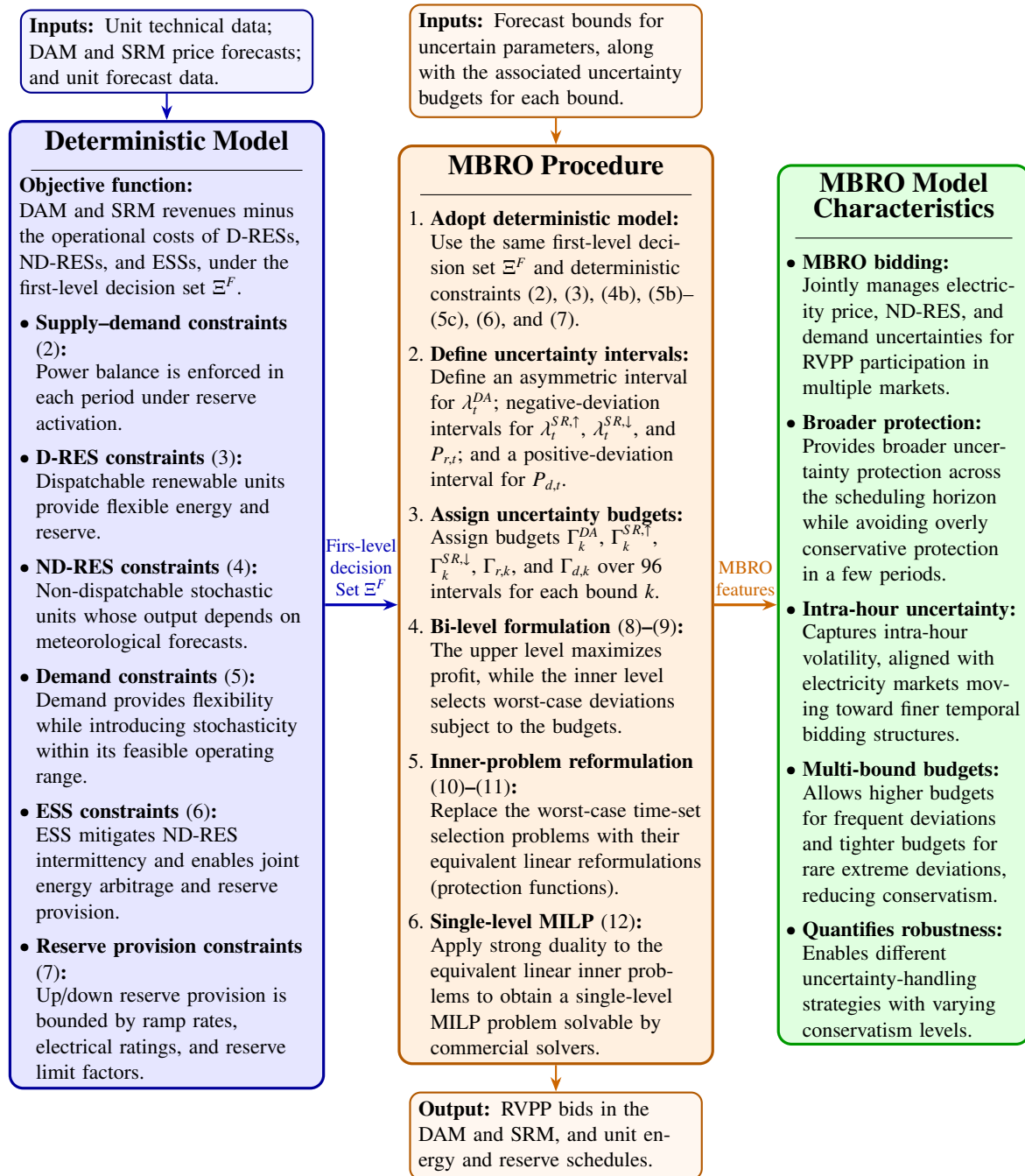


Figure 2: Procedure for developing the proposed MBRO framework and its key characteristics.

4. Case Studies

This section presents and discusses simulation results obtained with the proposed MBRO framework, with the aim of assessing how multiple sources of uncertainty affect the performance of an RVPP participating in the DAM and SRM. All experiments were executed on a Dell XPS laptop (Intel i7-1165G7, 2.8 GHz, 16 GB RAM) using CPLEX within GAMS 39.1.1.

4.1. System Description and MBRO Algorithm Parametrization

To account for the heterogeneity of the assets that may comprise an RVPP, and without loss of generality, the case study considers an RVPP located in Spain composed of a hydro plant, a wind farm, a solar PV plant, a Li-ion ESS, and a demand. Forecast data for the uncertain inputs (namely, wind and solar PV generation, demand consumption, DAM electricity price, and up/down SRM prices) are derived from historical records for November 2025 reported by [3]. This one-month period is used because quarter-hourly market data have only recently become available for Spain; the proposed framework is not tied to this window and can be readily applied to longer datasets as they become available. The corresponding uncertainty bounds are illustrated in Figure 3. For each uncertain parameter, three bounds ($k = 1, 2, 3$) are defined: $k = 1$ represents the most likely deviation range around the forecast, while $k = 2$ and $k = 3$ capture progressively less likely (more extreme) deviations, depicted with lighter shading. The deviation levels and their associated budgets are user-defined robustness settings. In practice, an RVPP operator can set them based on (i) operational experience and risk *appetite* from prior market participation, and/or (ii) calibration against historical forecast-error distributions for each uncertain input (e.g., selecting deviation bounds and allocating larger budgets to more likely bounds and smaller budgets to rarer extremes). A systematic procedure to identify “best-fit” bounds/budgets for a specific portfolio is an important topic but is outside the scope of this paper.

The technical characteristics of the RVPP assets are summarized in Table 2 and are taken from [31, 32]. Table 3 reports the uncertainty budgets associated with the bounds in Figure 3 for: (i) the proposed MBRO model with a 15-minute bidding resolution, (ii) a classic RO model with 15-minute resolution, and (iii) an RO model with hourly resolution. In the MBRO formulation, the sum of the budgets over all bounds ($k = 1, 2, 3$) is constrained to lie within 0 to 96. Moreover, inner bounds are assigned larger budgets than outer bounds to reflect their higher likelihood (i.e., small deviations are more frequent than large deviations). In the RO model with 15-minute resolution, the budget varies from 0 to 96, where larger values represent more conservative operation by allowing more periods to reach their worst-case realizations. In the hourly RO model, the corresponding budget ranges from 0 to 24, spanning the deterministic case (0) to the most conservative case (24), in which all hours may simultaneously attain worst-case values.

Based on these budgets, four strategies are considered for the RVPP operator: a deterministic strategy and three uncertainty-handling strategies (optimistic, balanced, and pessimistic). The following case studies are used to quantify the impact of the proposed MBRO approach, to benchmark it against the classic RO formulation, and to examine the effect of the market time resolution (15-minute versus hourly):

- **Case 1:** Evaluate the optimal operation of the RVPP units under the proposed MBRO model for the deterministic, optimistic, balanced, and pessimistic strategies.
- **Case 2:** Compare RVPP trading outcomes in the DAM and SRM using the RO model under hourly and 15-minute market resolutions across the different bidding strategies considered.
- **Case 3:** Compare trading decisions and the value of different uncertainties under the classic RO model and the proposed MBRO model for the different strategies.

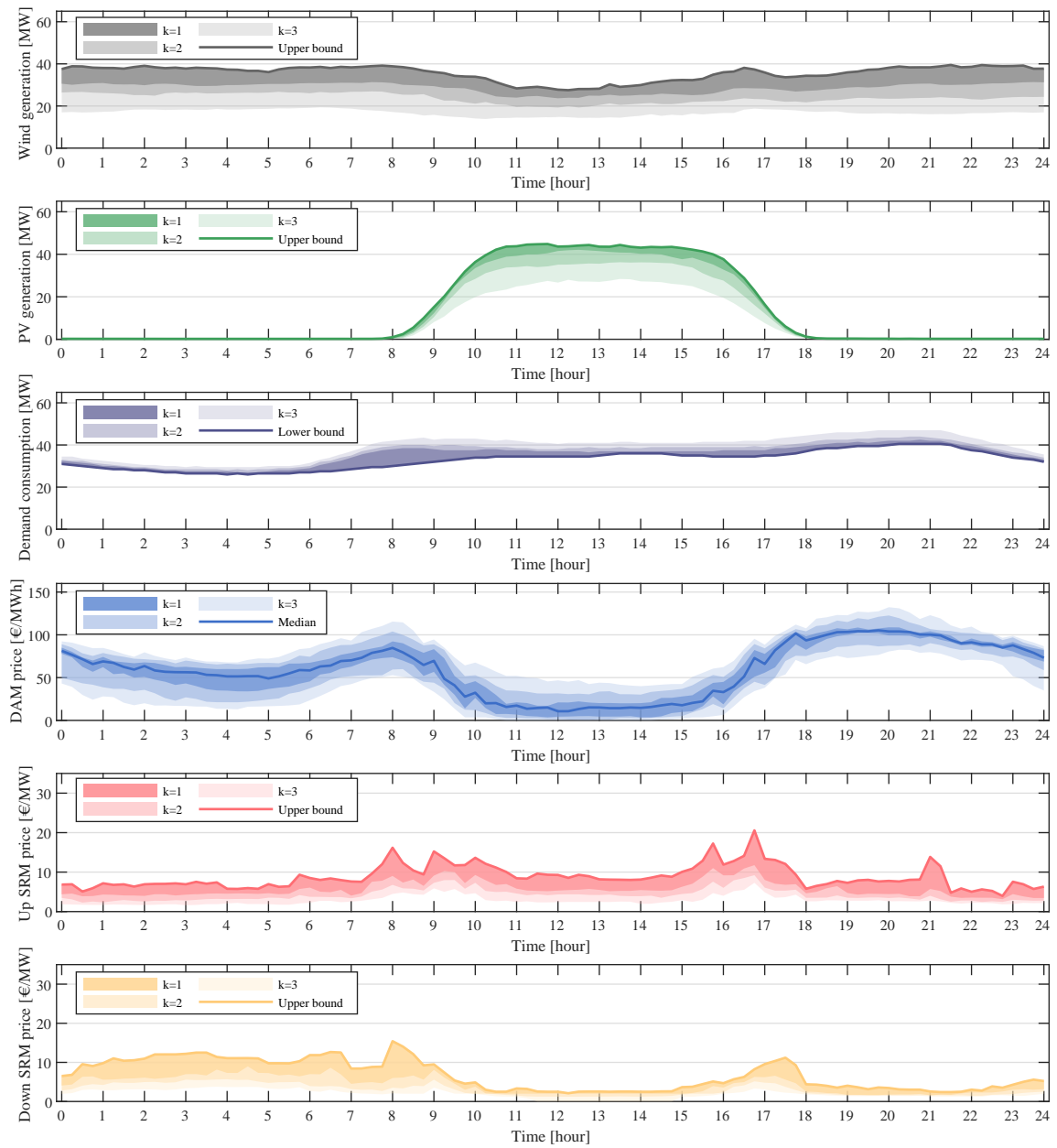


Figure 3: Uncertainty bound in multi-bound for different uncertainty handling strategies.

Table 2: RVPP units data.

Parameter	Solar PV	Wind farm	Hydro	ESS	Demand
$\bar{P}_u/\underline{P}_u$ [MW]	50/0	50/0	50/10	-	50/0
$R_u^\uparrow/R_u^\downarrow$ [MW/min]	20/25	15/20	10/10	10/10	3/3
$\beta_u^\uparrow/\beta_u^\downarrow$ [%]	5	5	50	100	0
$\bar{E}_u/\underline{E}_u$ [MWh]	-	-	480/-	30/3	-/750
\bar{P}_s^+/\bar{P}_s^- [MW]	-	-	-	10/10	-
η_s^+/η_s^- [%]	-	-	-	95/95	-
C_u [€/MWh]	10	15	12.5	30	-

Table 3: Uncertainty budgets for the RVPP operator's strategies in different robust frameworks.

Strategy	MBRO			RO 15-min	RO hourly
	$k = 1$	$k = 2$	$k = 3$		
Optimistic	16	4	2	16	4
Balanced	32	8	4	32	8
Pessimistic	48	12	6	48	12

4.2. Case 1

Figure 4 shows the energy schedules of the different RVPP units under a 15-minute market resolution for the different bidding strategies considered. In the deterministic strategy, the forecast values are treated as exact and uncertainties are neglected in the optimization problem, yielding the optimal unit dispatch under perfect-forecast assumptions. Wind and solar PV supply energy in the DAM according to their availability. In addition, the dispatchable hydro unit mainly generates during periods with high DAM prices, i.e., around 00:00–01:30, 06:45–08:45, and 16:45–24:00 (see the electricity price in Figure 3). The ESS charges mainly between 11:15 and 13:45, when solar PV availability is high, and discharges between 19:00 and 20:30, when DAM prices are higher. Under the optimistic strategy, uncertain parameters are allowed to deviate from their deterministic reference values according to uncertainty budgets defined in Table 3. Consequently, the scheduled energy of the units is affected, with lower wind and solar PV generation and higher demand consumption in the worst case. To compensate for the reduced output of the ND-RES, the hydro plant is scheduled for more periods than in the deterministic strategy. For instance, hydro generation extends over 00:00–01:45, 06:15–09:15, and 17:00–24:00. For the more conservative balanced and pessimistic strategies, the RVPP operator accounts for higher volatility in ND-RES when determining the unit schedules. As a result, as expected, the RVPP trades lower energy in the DAM, with greater variability across periods. Moreover, the role of the hydro plant in mitigating ND-RES fluctuations becomes more pronounced, and this dispatchable unit is scheduled more frequently. For example, under the pessimistic strategy, hydro generation is scheduled over 00:00–02:30, 05:30–09:15, and 16:45–24:00. Additionally, under the pessimistic strategy, the ESS schedules charging and discharging over a wider time window than in the deterministic strategy to hedge against uncertainty. For example, the ESS charges during 11:30–14:45 and discharges during 18:45–21:30. Overall, the results in Figure 4 indicate that the proposed framework effectively captures the impact of uncertainty on RVPP scheduling at a 15-minute market resolution across different uncertainty-handling strategies.

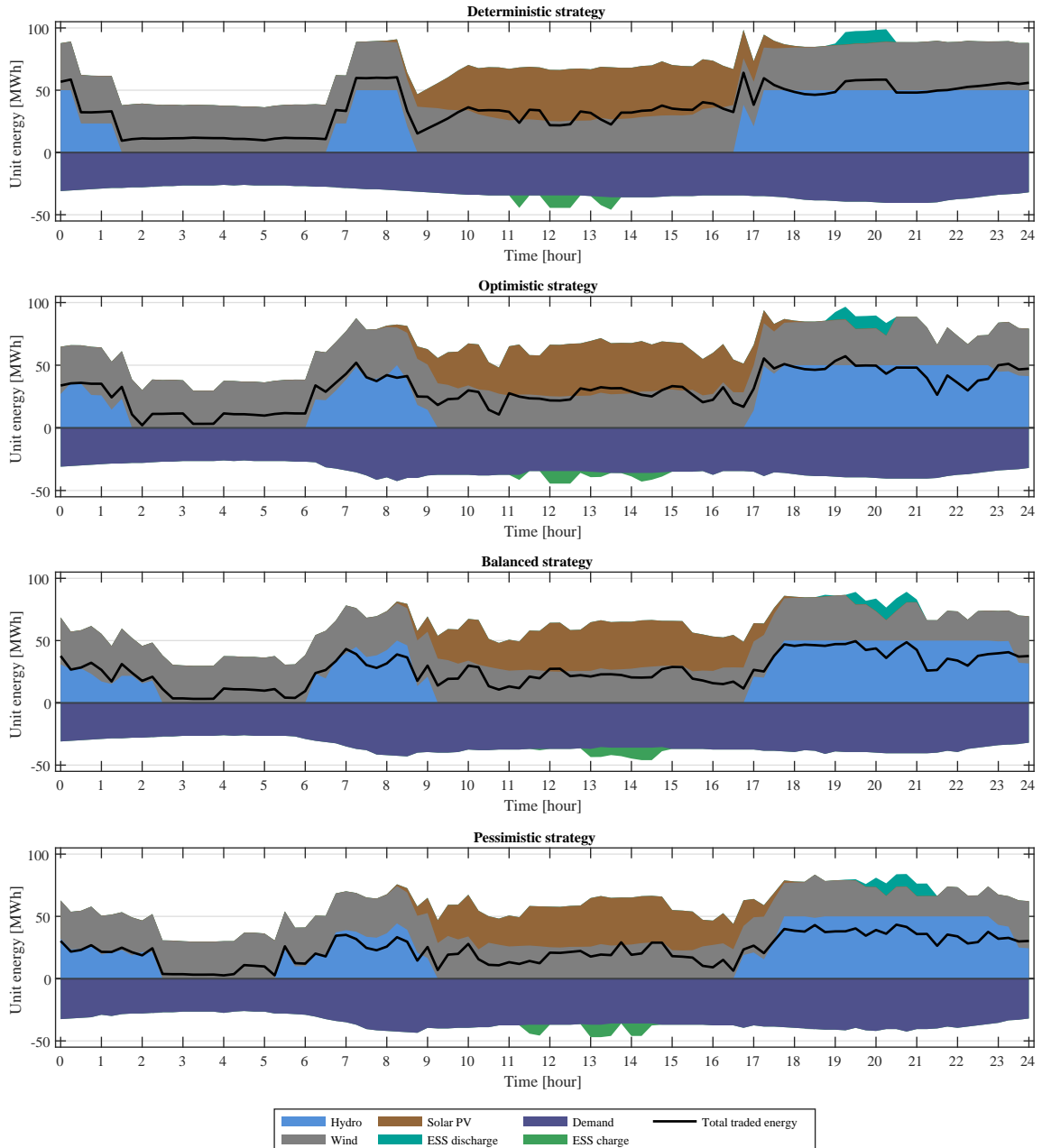


Figure 4: Case 1 – All RVPP unit energy in multi-bound for different uncertainty handling strategies.

Figure 5 shows the shares of up and down reserve provided by the RVPP units under a 15-minute market resolution for different bidding strategies. The results indicate that the ESS is one of the main providers of up reserve in the SRM. For instance, under the deterministic strategy, the ESS provides up reserve during several periods around 08:00–10:15, 15:30–17:30, and 21:00–21:15, when the up-SRM price is high (see Figure 3). A smaller share of up reserve is provided by the wind farm and the solar PV plant, mainly between 10:15 and 15:45. Regarding down reserve in the deterministic strategy, most of the down reserve is supplied by the hydro plant during the hours in which it is generating and can therefore curtail its output to provide down reserve. The ESS also provides down reserve in some periods, for example between 02:15 and 06:45. In addition, the wind farm and solar PV contribute a small share of down reserve depending on their availability to reduce production. It is worth noting that providing down reserve is generally easier than providing up reserve; accordingly, the RVPP offers down reserve in almost all scheduling periods. In contrast, up reserve is offered in fewer periods because the RVPP often prefers to allocate its resources to DAM energy trading rather than to up-reserve provision. Moreover, since DAM electricity prices are typically higher than SRM prices, energy trading tends to be a more reliable revenue source for the RVPP. Nevertheless, the RVPP still arbitrages between the two markets to enhance profitability. When adopting the optimistic strategy, and especially the more conservative balanced and pessimistic strategies, the RVPP tends to provide up reserve over a larger number of periods, typically with a lower reserve magnitude per period compared with the deterministic strategy. This behaviour can be explained by the fact that, once uncertainty is explicitly considered in the proposed MBRO framework, SRM prices may be adversely affected across many periods. Consequently, the RVPP adopts a more diversified reserve-bidding profile over time, reducing its exposure to price fluctuations in any single period and leading to a more robust and risk-averse strategy for profit maximization.

4.3. Case 2

Figure 6 compares the RVPP trading outcomes obtained with the *classic* RO model under hourly and 15-minute market resolutions across different uncertainty-handling strategies. Overall, the 15-minute formulation captures intra-hour trading dynamics that are inherently smoothed in the hourly framework, leading to more realistic and granular bidding decisions. Adopting alternative uncertainty-handling strategies can even change the trading direction in specific periods. For instance, under the balanced strategy the RVPP becomes a net buyer during 09:15–09:30 in the 15-minute market, while the hourly model does not reflect this change.

Table 4 compares the normalized absolute differences between the hourly and 15-minute schedules of RVPP traded energy in the DAM and traded up/down reserve in the SRM, for different uncertainty-handling strategies. For each hour, the hourly schedule is mapped to its four corresponding 15-minute periods; absolute deviations are computed period by period, summed over the full horizon, and then normalized by the total traded quantity in the hourly schedule. Larger percentages indicate stronger intra-hour variability captured by the 15-minute formulation but smoothed in the hourly formulation. In the deterministic strategy, this leads to normalized differences of 18.0%, 64.4%, and 15.6% for traded energy, up reserve, and down reserve, respectively. When uncertainty is considered (optimistic, balanced, and pessimistic strategies), the normalized differences do not increase monotonically; however, a generally increasing tendency is observed toward more conservative settings. For instance, under the pessimistic strategy the normalized differences reach their maximum values of 34.2%, 65.6%, and 16.3%. A key reason is that in more conservative strategies the RVPP typically trades less energy and reserve, so a given absolute mismatch between 15-minute and hourly schedules translates into a larger normalized deviation.

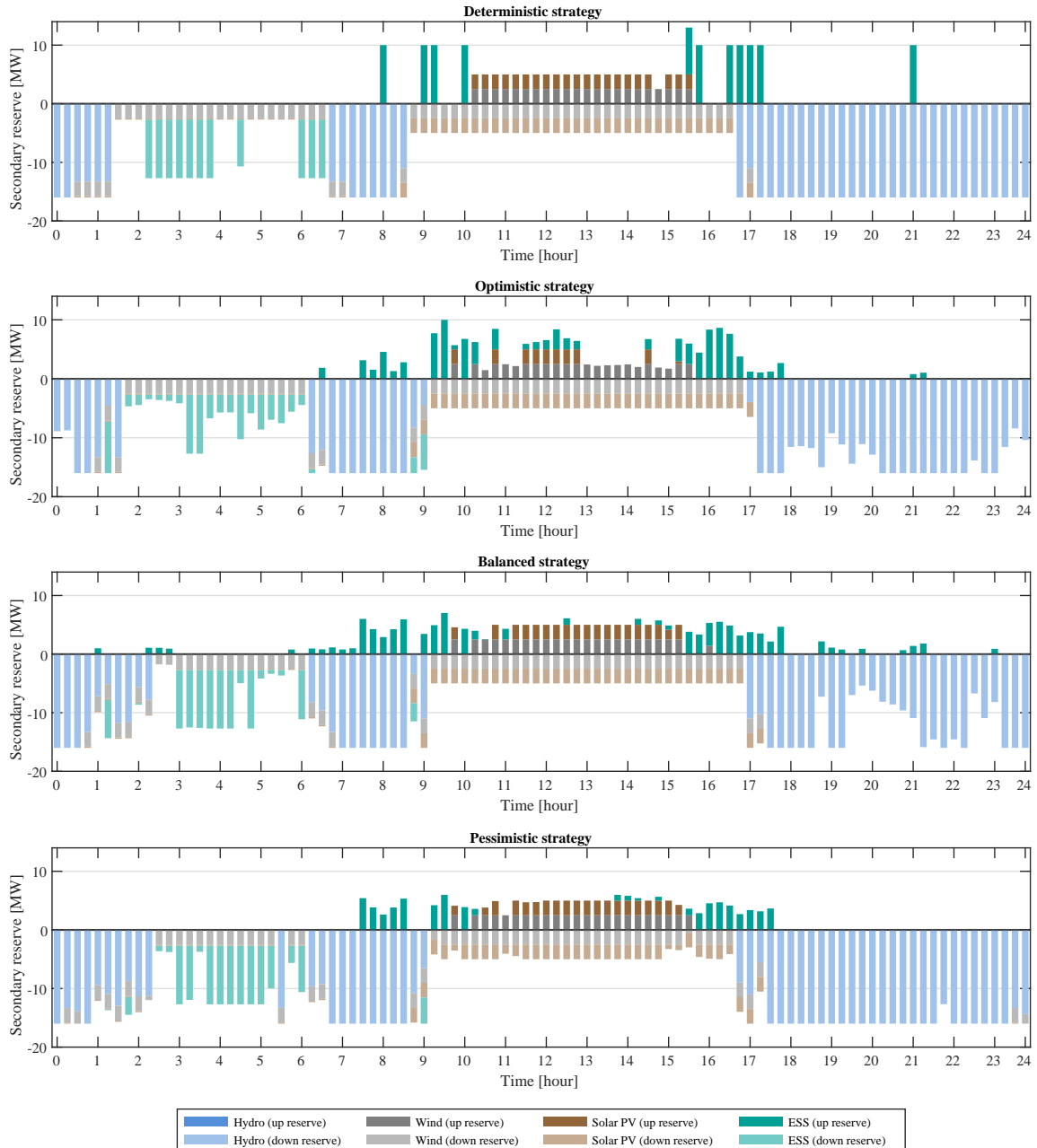


Figure 5: Case 1 – All RVPP unit reserve in multi-bound for different uncertainty handling strategies.

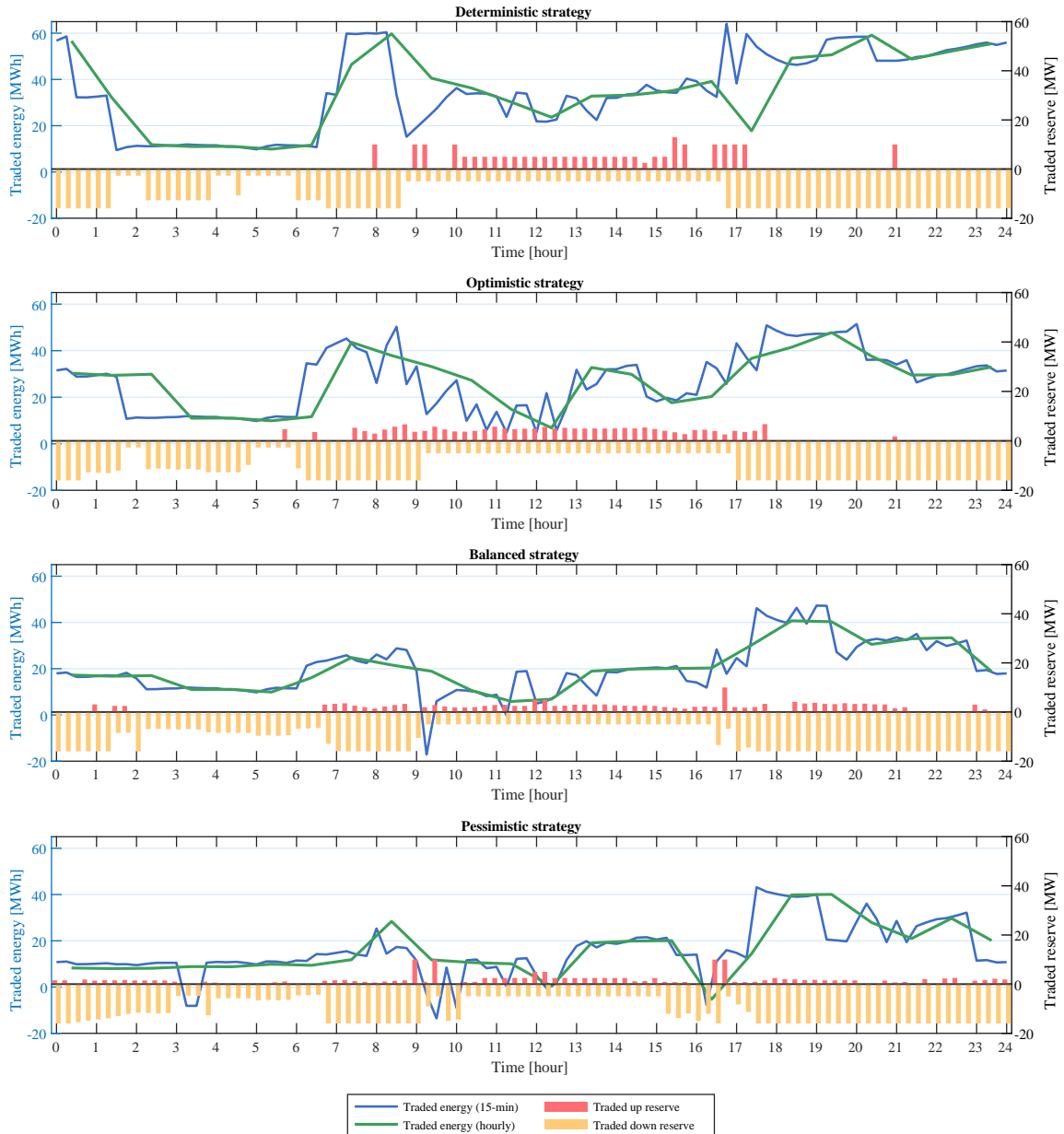


Figure 6: Case 2 – Total traded energy and reserve of RVPP in hourly and 15 min for different uncertainty handling strategies.

Table 4: Normalized absolute differences (%) between hourly and 15-minute traded energy in the DAM and up/down reserve in the SRM, for different uncertainty-handling strategies.

Strategy	Energy [%]	Up reserve [%]	Down reserve [%]
Deterministic	18.0	64.4	15.6
Optimistic	20.7	28.7	10.1
Balanced	18.7	59.5	11.1
Pessimistic	34.2	65.6	16.3

4.4. Case 3

Figure 7 compares the DAM price and the up/down SRM prices obtained with the proposed MBRO framework and the *classic*, single-bound RO model (referred to as SB in the results depicted below) under different uncertainty-handling strategies, considering 15-min market resolution. Overall, the RO formulation produces more frequent and abrupt deviations in both DAM and SRM prices. For instance, under the optimistic strategy, the DAM price in period 1:45–2:00 deviates downward by about 70% relative to the median value. Similar sharp negative DAM deviations appear in other periods, such as 17:45–20:00, 20:45–21:00, 22:30–23:00, and 23:15–23:30. In contrast, under the proposed MBRO framework, price deviations are distributed across multiple bounds, so moderate deviations occur more often while extreme deviations are less frequent, yielding a less conservative and more realistic representation of market prices. For example, in the optimistic strategy, the MBRO model allows low deviations in 16 periods, medium deviations in 4 periods, and high deviations in only 2 periods (see Table 3). As the bidding strategy becomes more conservative (balanced and pessimistic), price deviations occur in more periods in both formulations. Nevertheless, a clear difference remains: the single-bound RO model tends to push prices to their worst-case values more often, resulting in very conservative trajectories with abrupt jumps, whereas the MBRO model yields smoother behavior, with frequent low deviations and relatively rare extreme deviations.

Figure 8 compares the energy generation and consumption of the uncertainty-affected RVPP units obtained with the proposed MBRO framework and the classic RO model under different uncertainty-handling strategies. In the RO model, uncertainty is represented through a single worst-case realization, which translates into only acute decreases in wind farm and solar PV production and steep increases in demand consumption. For example, under the optimistic strategy, the wind farm output exhibits negative deviations in periods 0:15–0:45, 8:00–8:15, and 20:15–23:15, with deviations ranging from 55.9% to 59.1% relative to the upper forecast bound. In contrast, the proposed MBRO framework spreads deviations across multiple bounds, so low deviations occur more frequently and very sharp deviations occur less often. When moving from the optimistic to the balanced and pessimistic strategies, the RO model becomes increasingly conservative, driving uncertain generation/consumption close to their worst-case levels in most periods. By comparison, the proposed MBRO approach remains less conservative, with uncertainty primarily reflected through low and medium deviations and with extreme deviations appearing in relatively few periods.

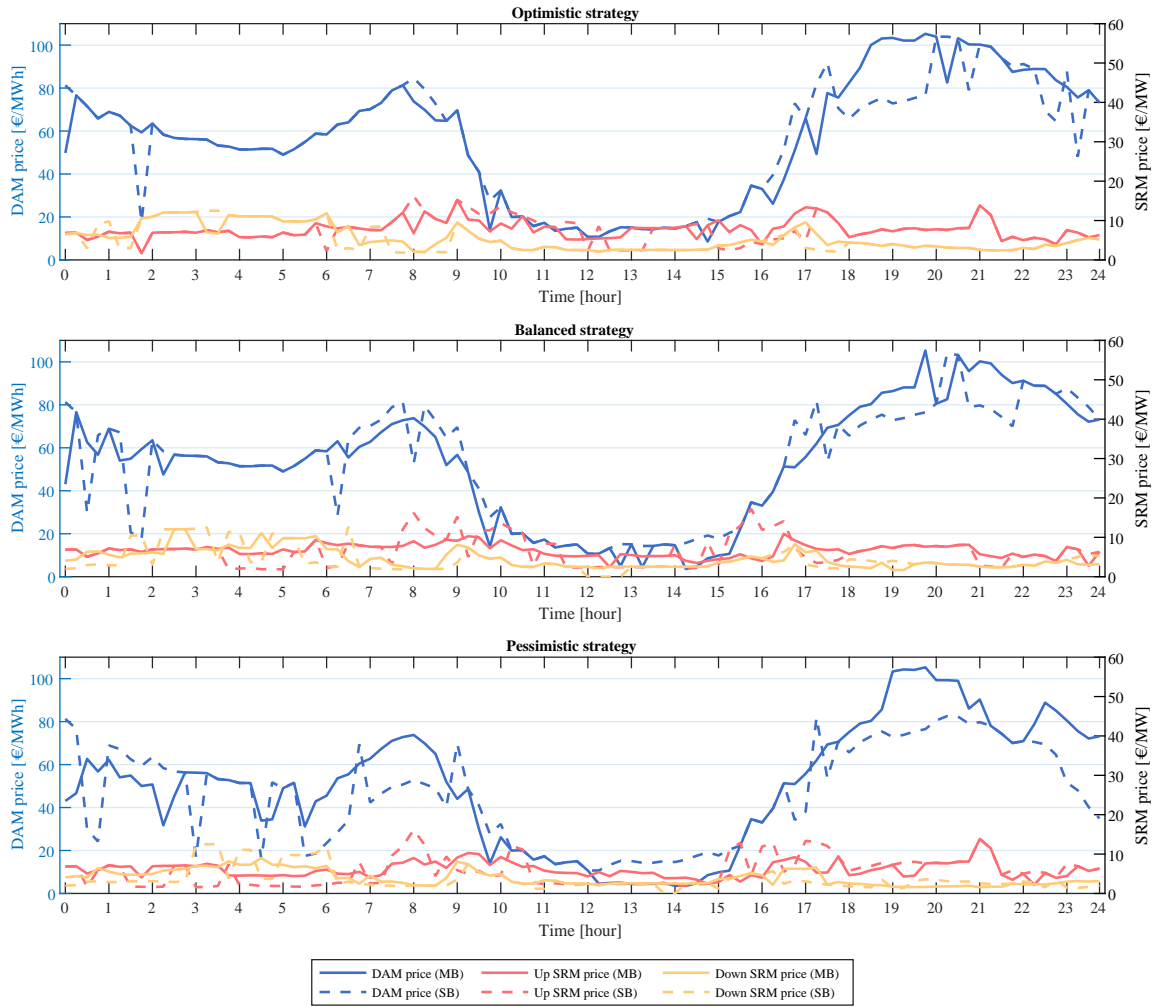


Figure 7: Case 3 - Electricity price in multi-bound (MB) and single-bound (SB) for different uncertainty handling strategies.

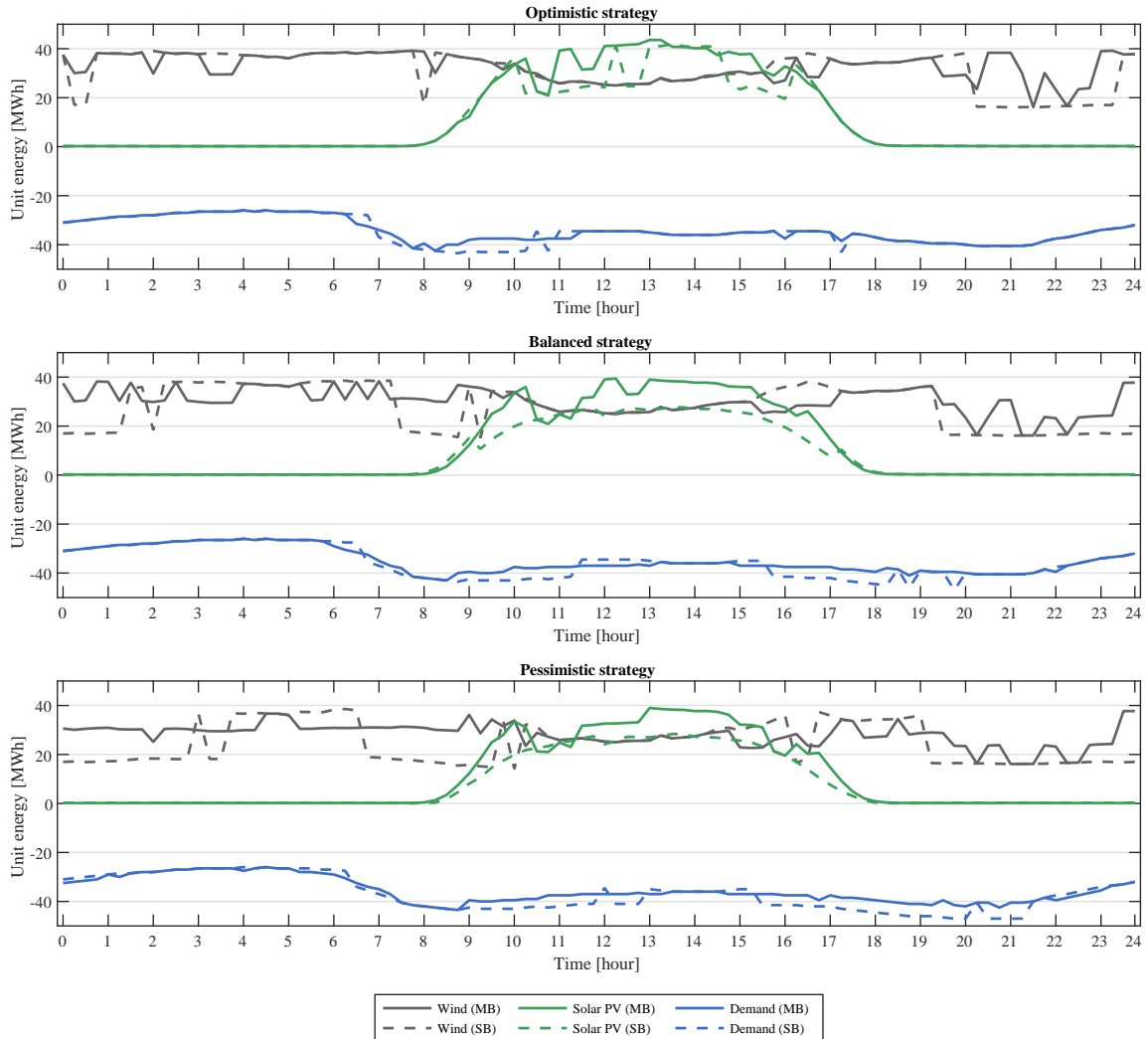


Figure 8: Case 3 – Unit energy in multi-bound and single-bound for different uncertainty handling strategies.

Figure 9 compares the traded energy of the RVPP obtained with the proposed MBRO framework and the classic RO model under different uncertainty-handling strategies. The traded reserve of the RVPP under the proposed MBRO framework is also shown in the figure. The traded reserve of the RVPP under the RO model, which was previously reported in Figure 6, is omitted here to avoid cluttering the figure. Overall, the RO approach leads to a much more conservative trading strategy for the RVPP in both the DAM and the SRM compared to the MBRO approach, confirming the observations discussed above.

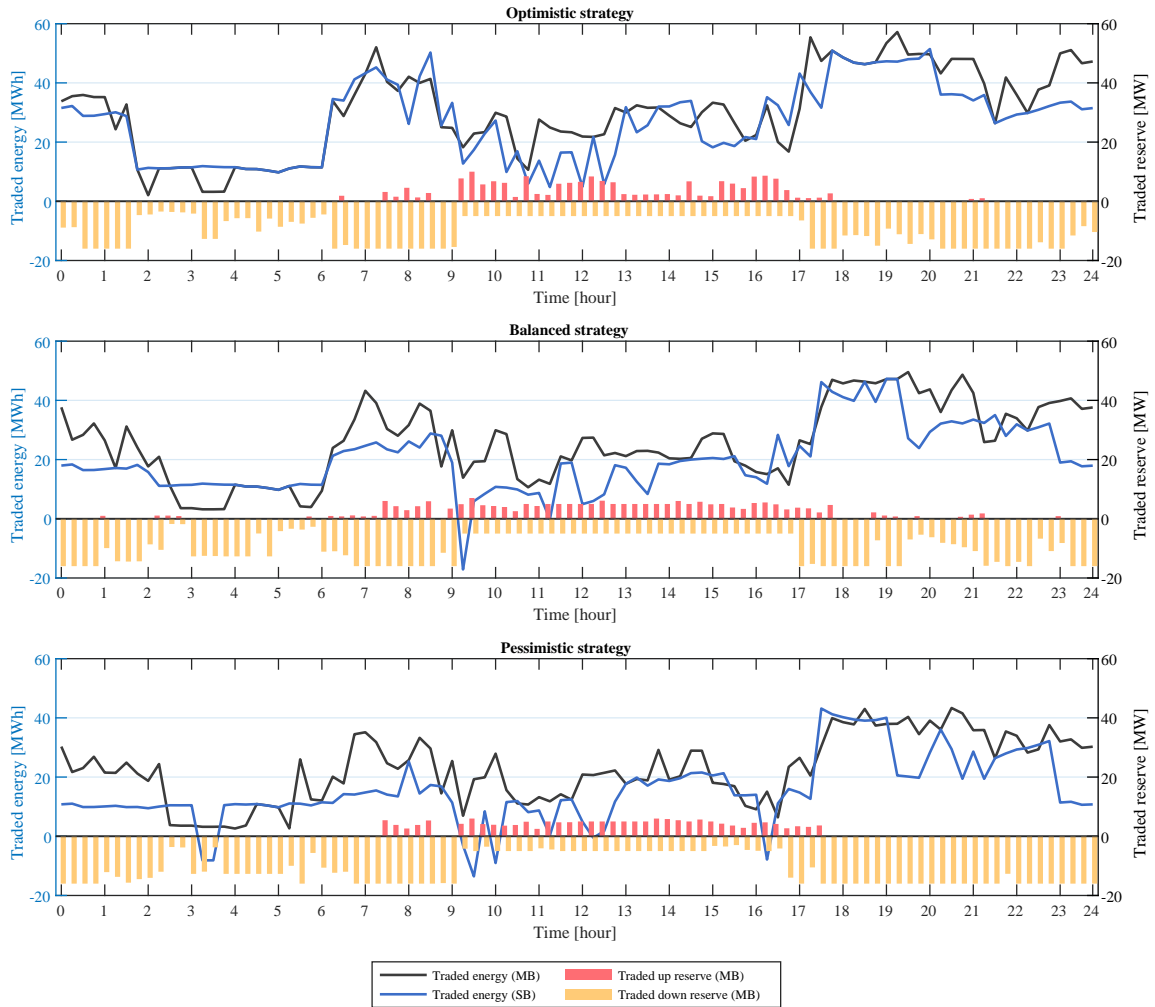


Figure 9: Case 3 – Total traded energy and reserve of RVPP in multi-bound and single-bound for different uncertainty handling strategies.

Table 5 compares the economic results of RVPP participation in the DAM and SRM, obtained using the proposed MBRO framework and the classic RO model under different uncertainty-handling strategies. The table reports the revenue from trading energy and reserve, the operation cost of RVPP units, the robust cost (i.e., the third line in the objective function (12a)), and the resulting profit, defined as revenue minus the operation and robust costs. It also reports the computational time of the simulations. Overall, the MBRO model returns higher profit and lower robust cost than the RO model across all uncertainty-handling strategies. To avoid inflated relative improvements when the RO profit is small, we normalize the profit difference by the RO optimistic profit (constant denominator across strategies). With this normalization, the MBRO profit under the optimistic, balanced, and pessimistic strategies is 24.9%, 42.8%, and 49.2% higher than that of the RO model, respectively. Moreover, the robust cost of the MBRO model is lower than that

Table 5: RVPP economic results in multi-bound and single-bound for different uncertainty handling strategies.

Model	Strategy	Profit [k€]	Revenue [k€]	Operation cost [k€]	Robust cost [k€]	Computational time [s]
SB approach	Optimistic	19.85	46.71	20.98	5.88	3.0
	Balanced	9.35	36.37	19.22	7.80	6.5
	Pessimistic	2.45	28.55	17.76	8.34	4.7
MB approach	Optimistic	24.81	51.01	21.89	4.31	59.5
	Balanced	17.85	44.87	20.73	6.29	38.8
	Pessimistic	12.22	39.78	19.93	7.63	17.9

of the RO model; under the optimistic, balanced, and pessimistic strategies, the corresponding reductions are 26.7%, 19.3%, and 8.5%, respectively. Finally, within the RO model, adopting the more conservative balanced and pessimistic strategies (relative to the optimistic strategy) reduces the RVPP profit by 52.9% and 87.6%, respectively. In contrast, the corresponding profit reductions in the MBRO approach are more moderate, at 28.0% and 50.7%. Regarding the computational time, the RO approach typically solves in less than 10 seconds for all uncertainty-handling strategies. The proposed MBRO approach requires higher computational effort, but for the considered RVPP it is usually solved in less than 1 minute across the different strategies. This comparison indicates that, while the MBRO approach provides greater flexibility for RVPP operators to handle multiple sources of uncertainty, its computational burden remains moderate and does not increase excessively compared to the simpler RO approach. Therefore, the proposed MBRO framework is efficient and suitable for performing multiple analyses before submitting the final RVPP bid to the market. These results highlight the effectiveness of the proposed MBRO approach for DAM and SRM participation. In comparison, the RO model leads to overly conservative solutions that may cause substantial profit reductions in market participation.

5. Conclusion

This paper proposes an MBRO framework for the optimal bidding of RVPP in energy and reserve markets, designed to align with the ongoing shift toward higher temporal market resolution (e.g., quarter-hourly scheduling). By deriving an MILP reformulation of the problem, the proposed method provides a mechanism to manage multiple uncertainties, including electricity prices, ND-RES production, and demand, with greater flexibility than classic approaches. Unlike standard RO, the MBRO framework allows for granular control over intra-hourly uncertainty exposure, ensuring protection across a wider range of time intervals without resorting to overly conservative worst-case assumptions. Three main remarks can be drawn from the results of the case studies presented and discussed. First, operational analysis demonstrates that D-RES effectively compensate for renewable fluctuations, while ESS and hydro units anchor the provision of ancillary services. Under uncertainty, the RVPP strategy shifts toward distributing reserve commitments across more intervals with lower individual magnitudes. Second, the comparison of market resolutions highlights the critical importance of granularity; the 15-minute model captures trading dynamics and flow reversals smoothed out by hourly frameworks, with volume discrepancies ranging from 18.0–34.2% for day-ahead energy, 28.7–65.6% for upward reserve, and 10.1–16.3% for downward reserve, based on the scenarios con-

sidered. Third, the proposed MBRO approach significantly outperforms classic RO by distinguishing between frequent but moderate deviations and rare, *extreme* anomalies. This strategic flexibility significantly increases profitability across different strategies while maintaining high computational efficiency, with solve times remaining under one minute for all cases considered.

Future work will extend this framework to explicitly model the correlations and non-linear interactions between different uncertainty parameters, further refining the representation of real-world market dynamics.

Appendix: Linear Reformulation of the Protection Functions

To reformulate the protection function of the objective function in (8) as a linear optimization problem (10), we utilize the following proposition based on [38].

Proposition 1: The value of the protection function in the third line of (8) is equivalent to the optimal objective value of the linear optimization problem (10).

Proof: The linear maximization problem defined in (10) maximizes its objective by setting the auxiliary variables corresponding to the largest coefficients to 1, contingent on constraint feasibility. Specifically, the optimal solution assigns exactly Γ_k^{DA} of the $z_{k,t}^{DA}$ variables to 1 for each bound k , provided that the limitation on the summation of the auxiliary variables $z_{k,t}^{DA}$ across all uncertainty bounds for any given time period in (10e) is satisfied. Analogous logic applies to the reserve variables, where $\Gamma_k^{SR,\uparrow}$ of the $z_{k,t}^{SR,\uparrow}$ variables and $\Gamma_k^{SR,\downarrow}$ of the $z_{k,t}^{SR,\downarrow}$ variables are set to 1, subject to similar summation limits in constraints (10f) and (10g), respectively. This mechanism is mathematically equivalent to the selection of the worst-case time sets $\{\mathcal{T}_k^{DA} \mid |\mathcal{T}_k^{DA}| = \Gamma_k^{DA}\}$, $\{\mathcal{T}_k^{SR,\uparrow} \mid |\mathcal{T}_k^{SR,\uparrow}| = \Gamma_k^{SR,\uparrow}\}$, and $\{\mathcal{T}_k^{SR,\downarrow} \mid |\mathcal{T}_k^{SR,\downarrow}| = \Gamma_k^{SR,\downarrow}\}$ utilized in the protection function in (8). ■

Additionally, to reformulate the protection function of the ND-RES constraint in (9b) as a linear optimization problem (11), we utilize the following proposition.

Proposition 2: The value of the protection function in the right-hand side of (9b) is equivalent to the optimal objective value of the linear optimization problem (11).

Proof: The linear maximization problem defined in (11) maximizes the deviation for the current period $t' = t$ by setting the auxiliary variable $z_{r,k,(t'=t)}$ to 1, contingent on constraint feasibility. Specifically, the optimal solution assigns $z_{r,k,(t'=t)} = 1$ for a chosen bound k if and only if the remaining uncertainty budget (calculated as $\Gamma_{r,k} - \sum_{t' \neq t} z_{r,k,t'}^*$) is sufficient, provided that the limitation on the summation of the auxiliary variable $z_{r,k,(t'=t)}$ across all uncertainty bounds in (11c) is satisfied. This mechanism is mathematically equivalent to determining whether period t can be included in the worst-case time set $\mathcal{T}_{r,k}$ for a specific bound k utilized in the protection function in (9b). ■

References

- [1] C. L. Prete, K. Palmer, M. Robertson, Time for a market upgrade? A review of wholesale electricity market designs for the future, *Energy Economics* (2025) 108640.
- [2] European Commission, Electricity Market Design, https://energy.ec.europa.eu/topics/markets-and-consumers/electricity-market-design_en (2025).
- [3] Red Eléctrica de España (REE), <https://www.ree.es/en> (2025).
- [4] Operador del Mercado Ibérico de Energía (OMIE), <https://www.omie.es/en> (2025).
- [5] European Network of Transmission System Operators for Electricity (ENTSO-E), Electricity Balancing Overview and Imbalance Settlement, https://www.entsoe.eu/network_codes/eb/ (2025).

- [6] C. Yang, X. Du, D. Xu, J. Tang, X. Lin, K. Xie, W. Li, Optimal bidding strategy of renewable-based virtual power plant in the day-ahead market, *Int. J. Electr. Power Energy Syst.* 144 (2023) 108557.
- [7] H. Gao, T. Jin, C. Feng, C. Li, Q. Chen, C. Kang, Review of virtual power plant operations: Resource coordination and multidimensional interaction, *Applied Energy* 357 (2024) 122284.
- [8] M. Kaiss, Y. Wan, D. Gebbran, C. U. Vila, T. Dragičević, Review on virtual power plants/virtual aggregators: Concepts, applications, prospects and operation strategies, *Renew. Sustain. Energy Rev.* 211 (2025) 115242.
- [9] J. Liu, J. Peng, H. Liu, J. Deng, X. Song, Two-stage robust optimization of a virtual power plant considering a refined demand response, *Energy* 322 (2025) 135560.
- [10] S. Wu, Y. Wang, L. Liu, Z. Yang, Q. Cao, H. He, Y. Cao, Two-stage distributionally robust optimal operation of rural virtual power plants considering multi correlated uncertainties, *International Journal of Electrical Power & Energy Systems* 161 (2024) 110173.
- [11] J. Feng, L. Ran, Z. Wang, M. Zhang, Optimal energy scheduling of virtual power plant integrating electric vehicles and energy storage systems under uncertainty, *Energy* 309 (2024) 132988.
- [12] Y. Li, Y. Deng, Y. Wang, L. Jiang, M. Shahidehpour, Robust bidding strategy for multi-energy virtual power plant in peak-regulation ancillary service market considering uncertainties, *International Journal of Electrical Power & Energy Systems* 151 (2023) 109101.
- [13] D. Falabretti, F. Gulotta, D. Siface, Scheduling and operation of RES-based virtual power plants with e-mobility: A novel integrated stochastic model, *Int. J. Electr. Power Energy Syst.* 144 (2023) 108604.
- [14] J. Cao, C. Xu, Z. Siqin, M. Yu, R. Diao, Scenario-driven distributionally robust optimization model for a rural virtual power plant considering flexible energy-carbon-green certificate trading, *Applied Energy* 379 (2025) 124904.
- [15] Y. Wang, W. Huang, H. Chen, Z. Yu, L. Hu, Y. Huang, Optimal scheduling strategy for virtual power plants with aggregated user-side distributed energy storage and photovoltaics based on CVaR-distributionally robust optimization, *Journal of Energy Storage* 86 (2024) 110770.
- [16] S. Mei, Q. Tan, A. Trivedi, D. Srinivasan, A two-step optimization model for virtual power plant participating in spot market based on energy storage power distribution considering comprehensive forecasting error of renewable energy output, *Applied Energy* 376 (2024) 124234.
- [17] D. Xiao, Z. Lin, H. Chen, W. Hua, J. Yan, Windfall profit-aware stochastic scheduling strategy for industrial virtual power plant with integrated risk-seeking/averse preferences, *Applied energy* 357 (2024) 122460.
- [18] M. Shafiekhani, A. Ahmadi, O. Homaei, M. Shafie-khah, J. P. Catalão, Optimal bidding strategy of a renewable-based virtual power plant including wind and solar units and dispatchable loads, *Energy* 239 (2022) 122379.
- [19] S. Afzali, M. P. Moghaddam, M. K. Sheikh-El-Eslami, R. Zamani, A flexibility-oriented bidding strategy for virtual power plants incorporating local energy communities: A bi-level stochastic-robust methodology, *Applied Energy* 399 (2025) 126355.
- [20] Y. Ma, Z. Li, R. Liu, B. Liu, S. S. Yu, X. Liao, P. Shi, Data-driven interval robust optimization method of VPP bidding strategy in spot market under multiple uncertainties, *Applied Energy* 384 (2025) 125366.
- [21] J. Wang, J. Xu, J. Wang, D. Ke, L. Yao, Y. Zhou, S. Liao, Two-stage distributionally robust offering and pricing strategy for a price-maker virtual power plant, *Applied Energy* 363 (2024) 123005.
- [22] Y. Zhu, N. Wei, J. Kang, Y. Tian, Low-carbon and robust economic scheduling of virtual power plants considering multiple uncertainties, *Sustainable Energy, Grids and Networks* (2025) 102104.
- [23] Y. Shang, X. Li, T. Xu, L. Cui, Uncertainty-output virtual power plant participates in multi-electricity market considering the improved shapley value distribution method, *International Journal of Electrical Power & Energy Systems* 165 (2025) 110462.
- [24] J. Feng, L. Ran, Z. Wang, M. Zhang, Optimal bidding strategy for virtual power plant in multiple markets considering integrated demand response and energy storage, *Journal of Energy Storage* 124 (2025) 116706.
- [25] H. Du, J. Hu, Y. Fang, D. Xie, Optimal bidding strategy for virtual power plant participating in joint energy and reserve market considering physical-economic feasible operation region, *Energy* (2025) 138410.
- [26] Z. Siqin, R. Diao, M. Zhao, Two-stage distributionally robust bidding strategies for multi-energy virtual power plants in energy, reserve and carbon markets, *Energy* (2025) 137455.
- [27] M. Esfahani, A. Alizadeh, B. Cao, I. Kamwa, M. Xu, A stochastic-robust aggregation strategy for VPP to participate in the

frequency regulation market via backup batteries, *Journal of Energy Storage* 98 (2024) 113057.

[28] E. Nokandi, M. Vahedipour-Dahraie, S. R. Goldani, P. Siano, A three-stage bi-level model for joint energy and reserve scheduling of VPP considering local intraday demand response exchange market, *Sustainable Energy, Grids and Networks* 33 (2023) 100964.

[29] A. G. Zamani, A. Zakariazadeh, S. Jadid, Day-ahead resource scheduling of a renewable energy based virtual power plant, *Applied Energy* 169 (2016) 324–340.

[30] H. Nemati, P. Sánchez-Martín, Á. Ortega, L. Sigrist, E. Lobato, L. Rouco, Flexible robust optimal bidding of renewable virtual power plants in sequential markets under asymmetric uncertainties, *Sustainable Energy, Grids and Networks* (2025) 101801.

[31] H. Nemati, P. Sánchez-Martín, A. Baringo, Á. Ortega, Single-level flexible robust optimal bidding of renewable-only virtual power plant in energy and secondary reserve markets, *Energy* (2025) 136421.

[32] H. Nemati, P. Sánchez-Martín, Á. Ortega, L. Sigrist, L. Rouco, Integration of concentrated solar power plants in renewable-only VPP with electrical and thermal demands: A two-stage robust bidding approach, *Journal of Energy Storage* 141 (2026) 119265.

[33] Q. Li, F. Dong, B. Jiang, J. Liu, P. Yan, D. Yu, Risk-averse co-optimization of virtual power plants in multi-markets considering scheduling costs and uncertainties of controllable loads, *Applied Energy* 409 (2026) 127496.

[34] W. Li, F. Dong, Z. Ji, P. Wang, Internal and external coordinated distributionally robust bidding strategy of virtual power plant operator participating in day-ahead electricity spot and peaking ancillary services markets, *Applied Energy* 386 (2025) 125514.

[35] Z. Yuanyuan, Z. Huiru, L. Bingkang, Distributionally robust comprehensive declaration strategy of virtual power plant participating in the power market considering flexible ramping product and uncertainties, *Applied Energy* 343 (2023) 121133.

[36] J. Wang, V. Ilea, C. Bovo, N. Xie, Y. Wang, Optimal self-scheduling for a multi-energy virtual power plant providing energy and reserve services under a holistic market framework, *Energy* 278 (2023) 127903.

[37] C. Büsing, F. D'andreagiovanni, New results about multi-band uncertainty in robust optimization, in: *International symposium on experimental algorithms*, Springer, 2012, pp. 63–74.

[38] D. Bertsimas, M. Sim, The price of robustness, *Operations Research* 52 (1) (2004) 35–53.

[39] M. Carrión, J. M. Arroyo, A computationally efficient mixed-integer linear formulation for the thermal unit commitment problem, *IEEE Transactions on power systems* 21 (3) (2006) 1371–1378.

[40] Z. Zhang, M. Zhou, Z. Wu, S. Liu, Z. Guo, G. Li, A frequency security constrained scheduling approach considering wind farm providing frequency support and reserve, *IEEE Transactions on Sustainable Energy* 13 (2) (2022) 1086–1100.

[41] S. Yin, J. Wang, Z. Li, X. Fang, State-of-the-art short-term electricity market operation with solar generation: A review, *Renewable and Sustainable Energy Reviews* 138 (2021) 110647.

[42] C. A. Floudas, *Nonlinear and mixed-integer optimization: fundamentals and applications*, Oxford University Press, 1995.